Pharmaceutical Research, Vol. 24, No. 6, June 2007 (© 2007)
DOI: 10.1007/s11095-006-9223-y

Expert Review

Functionalized Micellar Systems for Cancer Targeted Drug Delivery

Damon Sutton,[1] Norased Nasongkla,[1,2] Elvin Blanco,[1] and Jinming Gao[1,3]

Received November 6, 2006; accepted December 21, 2006; published online March 24, 2007

Abstract. Polymer micelles are rapidly becoming a powerful nanomedicine platform for cancer therapeutic applications due to their small size (10–100 nm), *in vivo* stability, ability to solubilize water insoluble anticancer drugs, and prolonged blood circulation times. Recent data from clinical trials with three micelle formulations have highlighted these and other pharmacokinetic advantages with reduced systemic toxicity and patient morbidity compared to conventional drug formulation. While the initial anti-tumor efficacy of these systems seems promising, a strong research impetus has been placed on micelle functionalization in order to achieve tumor targeting and site-specific drug release, with the hope of reaching a more pronounced tumor response. Hence, the purpose of this review is to draw attention to the new developments of multi-functional polymer micelles for cancer therapy with special focus on tumor targeting and controlled drug release strategies.

KEY WORDS: active targeting; cancer nanomedicine; micelle pharmacokinetics; polymer micelles; responsive drug release.

INTRODUCTION

Recently, polymer micelles have gained considerable attention as a versatile nanomedicine platform with greatly improved drug pharmacokinetics and efficacious response in cancer treatment. Typical chemotherapeutic agents have low water solubility, short blood half-lives, narrow therapeutic indices, and high systemic toxicity, which lead to patient morbidity and mortality while compromising the desirable therapeutic outcome of the drugs. Polymer micelles have been shown to increase the aqueous solubility of chemotherapeutic agents and prolong their *in vivo* half-lives with lessened systemic toxicity. This is demonstrated in early phases of clinical trials in Japan, Korea, and the United States (1–3).

Several excellent reviews are currently available in the literature on micellization behavior, drug encapsulation, and general use of micelles as drug delivery systems (4–13). The purpose of this review is to provide an updated, comprehensive review on recent breakthroughs and applications of polymer micelles for tumor-specific therapy. First, a brief overview on micelle structure and composition will be presented, followed by a summary on the clinical pharmacokinetics of "stealth" micelles. This will be followed by a comprehensive review of micelle systems consisting of additional functionality. Special emphasis will be placed on micellar systems that exploit unique molecular signatures on cancer cells for active targeting applications or responsive mechanisms (e.g. pH, temperature) for site-specific drug release.

MICELLE STRUCTURE AND COMPOSITION

Polymer micelles are composed of amphiphilic macromolecules that have distinct hydrophobic and hydrophilic block domains, with the structure of the copolymers usually being a di-block, tri-block, or graft copolymer. Within each copolymer system, aqueous exposure induces the hydrophobic and hydrophilic segments to phase separate and form nanoscopic supramolecular core/shell structures (Fig. 1). Depending on the relative size of the hydrophobic and hydrophilic segments and solvent conditions, Eisenberg *et al*. have demonstrated the formation of structures of many morphologies, including spheres, rods, vesicles, tubules, and lamellae (14–17). Although aggregates of different morphology may provide drastically different pharmacokinetic properties, as in the case of filamentous nanocarriers which can provide different flow behavior over spherical particles due to anisotropic alignment (18–20), most current applications have focused on spherical micelles and thus will be the subject of this review.

Many types of copolymers have been used for micelle formation, but the requirements of biocompatibility and oftentimes biodegradability have limited the choice of copolymers in clinical applications. Table I provides the names and structures of common copolymers for drug delivery applications. For the hydrophilic segment, the most commonly used polymer is polyethylene glycol (PEG) with a molecular weight of 2–15 kD. PEG is completely water

[1] Simmons Comprehensive Cancer Center, University of Texas Southwestern Medical Center at Dallas, 5323 Harry Hines Blvd., Dallas, Texas 75390, USA.
[2] Present address: Department of Biopharmaceutical Sciences and Pharmaceutical Chemistry, School of Pharmacy, University of California, San Fransisco, 513 Parnassus Avenue, Health Science East 1145 B, San Francisco, California 94143, USA.
[3] To whom correspondence should be addressed. (e-mail: jinming.gao@utsouthwestern.edu)

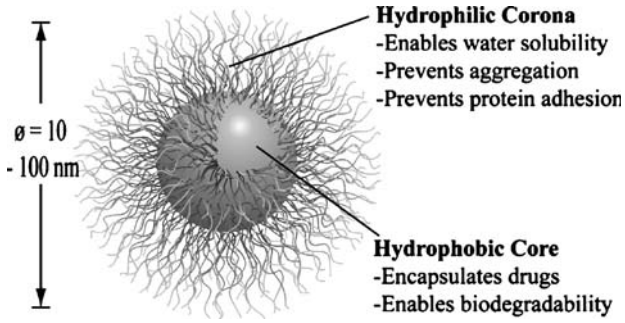

Fig. 1. Schematic illustration of the core-shell structure of a polymer micelle with intended functions of each component.

soluble, non-toxic, and uncharged, the latter property serving to lessen the possibility of undesired electrostatic interactions with plasma proteins. Other hydrophilic polymers such as poly(N-vinyl pyrrolidone) (PVP) (21) or poly(N-isopropyl acrylamide) (pNIPAM) (22–24) have also been used to form the micelle corona layer. For the hydrophobic segments, the most common materials are hydrophobic polyesters, but other materials, such as polyethers, polypeptides, or poly(β-amino ester) have also been used. Polyesters and polyamides can undergo hydrolytic and enzyme-catalyzed degradations, respectively, and are considered biodegradable. As an example of a micelle forming copolymer, Pluronic is a ternary copolymer of PEG and poly(propylene oxide) (PPO) oriented in a PEG-PPO-PEG configuration. Upon micellization, the hydrophobic PPO segments form the core while the PEG segments form the corona.

The core-shell structure of polymer micelles affords several advantages for drug delivery applications. Firstly, drug encapsulation within the micelle core allows for solubilization of water insoluble drugs. For example, the water solubility of paclitaxel can be increased by several orders of magnitude from 0.0015 to 2 mg/ml through micelle incorporation (25). Secondly, micelles have prolonged blood half-lives because PEG prevents opsonization, effectively reducing micelle uptake by the reticuloendothelial system (RES) (26,27). Thirdly, their small size (10–100 nm) makes them suitable for injection and enhanced tumor deposition due to the enhanced permeability and retention (EPR) effect stemming from the leakiness of tumor vasculature (28). Finally, their chemistry allows for the development of multifunctional modalities that can enhance micelle accumulation in cancerous tissues and facilitate drug internalization inside cancer cells.

CLINICAL PHARMACOKINETICS OF STEALTH MICELLES

Currently, clinical data on three polymer micelle systems, SP1049C, NK911, and Genexol-PM have been reported (1–3). All three are 'stealth' micelle formulations, i.e. they all have stabilizing PEG coronas to minimize opsonization of the micelles and maximize blood circulation times. SP1049C is formulated as doxorubicin (DOX)-encapsulated Pluronic micelles, NK911 is DOX-encapsulated micelles from a copolymer of PEG and DOX-conjugated poly(aspartic acid), and Genexol-PM is a paclitaxel-encapsulated PEG-PLA micelle formulation. The pharmacokinetic results of the three formulations are summarized in Table II. These data were compared to free DOX (doxorubicin hydrochloride) (29) as well as liposome-delivered DOX (Doxil®) (30) and Cremophor® EL-delivered paclitaxel (31).

Comparison among the various formulations of doxorubicin reveals several distinguishing characteristics. Free DOX has an elimination phase half-life ($t_{1/2,\beta}$), or physiological excretion half-life, of 48 min. Both polymer micelle formulations roughly triple the half-life, bringing it to a range of 2.3–2.8 h whereas the liposomal form greatly increases the half-life to 45.9 h. Since different formulations are evaluated using differing compartmental models, quantitative comparison of half-lives between formulations can be difficult. However, comparison of the common parameters, such as clearance rates, is more illustrative. The drug clearance rates (C_L) from different formulations serve to highlight further differences. The C_L of the free DOX is 14.4 ± 5.6 ml/(min kg), while pluronic micelles did not significantly improve the C_L value (12.6 ml/(min kg)), presumably due to the low stability of Pluronic micelles which may rapidly dissociate upon dilution. In contrast, DOX encapsulation within the more stable NK911 micelles reduced the clearance rate by almost half (6.7 ± 1.1 ml/(min kg)). Liposomal DOX has a remarkably decreased clearance rate (0.02 ml/(min kg)), which is two orders of magnitude smaller than either micellar formulation. This very slow clearance rate may at first appear ideal, however several factors indicate otherwise. Firstly, the extremely low volume of distribution (V_{ss} = 0.08 l/kg) suggests that liposomal DOX may remain in the bloodstream and not extravasate into tumor tissue as widely as comparable micelles. Micelles, on the other hand, have been shown to accumulate more readily inside tumors compared to liposomes, primarily due to the smaller micellar size (32). Interestingly, another study found that the high blood residence times of liposomally formulated DOX may cause increased levels of stomatitis (33).

The other major chemotherapeutic drug which has been clinically used in micelles is paclitaxel (Taxol®), a potent anticancer drug with very low water solubility (1.5 μg/cc). As a result, this agent already requires administration with a surfactant carrier. Currently, the clinically approved carrier to solubilize the drug is Cremophor® EL, a polyethylene glycol modified castor oil. Though useful in drug administration, the delivery agent itself has negative side effects such as hypersensitivity reactions (HSR) and neuropathy. To overcome this limitation, an alternate delivery system using PEG-PLA micelles, Genexol-PM, has been developed.

Cremophor® EL and Genexol-PM formulations have similar drug pharmacokinetics at 230 mg/m^2 dose (Table II). Both have similar half-lives (8.9 ± 1.8 and 11.0 ± 1.9 h from Cremophor® EL and Genexol-PM, respectively), and clearance rates (3.9 ± 1.1 and 4.8 ± 1.0 ml/(min kg), respectively). However, the Genexol-PM formulation shows marked improvement in patient morbidity. None of the patients observed in the Genexol-PM trial showed HSRs. Moreover, a lower degree of myelosupression was observed in the Genexol-PM formulation than in the conventional one. Consequently, the PEG-PLA micelles allow for a consider-

Table I. Commonly Used Block Segments of Copolymers used in Micellar Drug Delivery

Copolymers	Abbreviations	Repeating Unit Structure
Corona segment		
Poly(ethylene glycol)	PEG, PEO	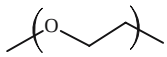
Poly(N-vinyl pyrrolidone)	PVP	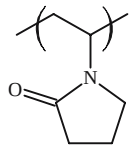
Poly(N-isopropyl acrylamide)	pNIPAM, NIPAM	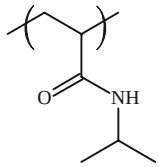
Core segment		
Polyethers		
Poly(propylene oxide)	PPO	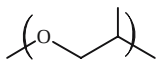
Polyesters		
Poly(L-lactide), Poly(D, L-lactide)	PLA, PDLLA*	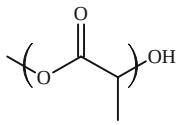
Poly(lactide-co-glycolide)	PLGA	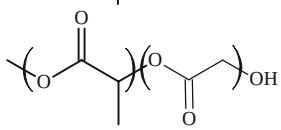
Poly(ε-caprolactone)	PCL	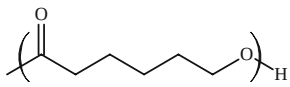
Poly(β-amino ester)		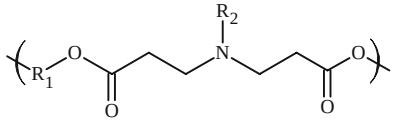
Polyamides		
Poly(L-histidine)	pHis	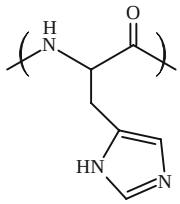
Poly(L-aspartic acid) derivatives	pAsp	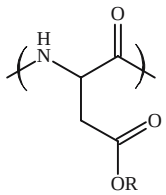
Poly(L-glutamic acid) derivatives	pGlu	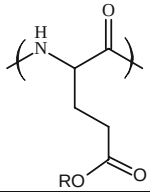

* Depending on stereochemistry

able increase in maximum tolerated dose (MTD) with an MTD of 390 mg/m^2 compared to 230 mg/m^2 for Cremophor® EL. A final interesting note is that in the Genexol-PM trial, two patients showed tumor response despite previous paclitaxel failure in their treatments (3).

Clinical data demonstrates the distinct pharmacokinetic advantages of micelle-delivered drugs over free drugs. All of the doxorubicin micelle formulations show improved half-lives, slower clearance rates and increased area under plasma concentration (AUC) values over unencapsulated doxorubicin. Polymer micelles have also shown advantages in paclitaxel delivery in that they minimize toxicity associated with more traditional delivery systems. These data underscore the therapeutic potential of polymer micelles to improve cancer therapy.

FUNCTIONALIZED POLYMER MICELLES

Although stealth micelles allow for passive accumulation inside tumors with leaky vasculature, the majority of these nanoparticles are still cleared by the RES system, resulting in short half lives and unwanted micelle deposition in the liver and spleen. Development of multifunctional micelles, either through conjugation of targeting ligands on the micelle surface or a triggered release mechanism, can lessen these problems by increasing particle/drug exposure to the tumor. Fig. 2 illustrates the different types of functionality that have been introduced to micelle structures.

LIGAND-TARGETED POLYMER MICELLES

Targeting ligands are conjugated to the corona of the micelle in order to induce specific targeting and uptake of the micelle by tumor cells. These ligands tend to fall into the categories of small organic molecules, carbohydrates, antibodies, and aptamers. Table III provides an overview of reported ligand-targeted micelle formulations.

Micelles with small organic molecules as targeting ligands. The receptor for folic acid is a cell-proliferation protein that is over-expressed in many types of cancer cells including ovarian, breast, brain, and lung (34–36). The expression levels in tumors have been reported to be 100–300 times higher than those observed in normal tissue (37). It is a glycosyl-phosphatidylinositol-anchored glycoprotein that has high binding affinity to folic acid (K_d 10^{-10} M). Yoo and Park exploited the folate receptor by functionalizing folic acid onto DOX-loaded PEG-PLGA micelles by covalently conjugating the ligand via its γ-carboxyl group (38). *In vitro* cytotoxicity studies of the folate-micelles against KB cells (human nasopharyngeal epidermal carcinoma cell line) showed enhancement in cell uptake and cytotoxicity over non-targeted micelles, with the IC_{50} of DOX/FOL micelles, DOX micelles and free DOX being 50, 70 and 75 μM, respectively. Despite this small increase in *in vitro* cytotoxicity, the targeted micelles showed marked improvement in *in vivo* antitumor efficacy with two times decrease in the growth rate compared to non-targeted micelle control. Folate targeting was also used by these researchers to produce a DOX-based micellar system that did not contain polymer in the core (39). These targeted micellar nanoaggregates are based on a folate-PEG-DOX system which is self-assembled through hydrophobic doxorubicin association. This strategy leads to larger particles of approximately 200 nm in diameter with drug loading content as high as 57% since the majority of the nanoparticle is constructed from drug. Similar to the PLGA system, the folate-PEG-DOX nanoaggregate system showed twofold increased cytotoxicity over non-targeted aggregates, and an improved anti-tumor efficacy by a 40% decrease in tumor volume over free drug administration.

Park *et al.* also used folic acid as a targeting ligand but with a different folate conjugation strategy. In this case, folic acid was attached to the hydrophobic end of PEG-PCL block copolymer. Paclitaxel was then encapsulated (40,41). While it is unusual to couple a targeting ligand to the hydrophobic portion of the micelle, the authors reported folate to be

Table II. Comparison of Clinical Pharmacokinetics for Different Micellar Nanocarriers and Corresponding Commonly Used Formulations

Formulation	Free DOX[a]	SP1049C[a]	NK911[a]	Doxil®[b]	Taxol®[c]	Genexol[c]
Drug	DOX	DOX	DOX	DOX	Paclitaxel	Paclitaxel
Carrier	DOX-HCl in 0.9% NaCl	Pluronic micelles, mixture of L61 and F127	PEG5k-pAsp$_{30}$-(DOX)$_{45micelles}$	PEG-stabilized liposome	Cremophor® EL	PEG-PLA
Diameter (nm)	–	22–27	40	80–90	–	20–50
No. Patients	8	26	23	14	34	21
$t_{1/2,\alpha}$ (min)	2.4 ± 0.9	6.0 ± 2.7	7.5 ± 0.7	84	21.8 ± 13.9	–
$t_{1/2,\beta}$ (h)	0.8 ± 1.1	2.4 ± 2.1	2.8 ± 0.3	45.9	8.9 ± 1.8	11.0 ± 1.9
$t_{1/2,\gamma}$ (h)	25.8 ± 11.4	50.2 ± 29.2	64.2 ± 8.9	–	–	–
V_{ss} (L/kg)	24 ± 12	–	14.9 ± 3.6	0.08	–	–
C_L (ml/(min kg))	14.4 ± 5.6	12.6 ± 0.6	6.7 ± 1.1	0.02	3.9 ± 1.1	4.8 ± 1.0
MTD (mg/m^2)	50	70	67	50	230	390
AUC μg h/ml	1.6 ± 1.1	1.8 ± 0.3	3.3 ± 0.4	902	25 ± 6.5	27.5 ± 8.2
Reference	(29)	(1)	(2)	(30)	(31)	(3)

[a] Reported pharmacokinetic data at dose of 50 mg/m^2.
[b] Only two doses were tested in this trial, 25 and 50 mg/m^2, the reported values are at 50 mg/m^2.
[c] Reported pharmacokinetic data at 230 mg/m^2.

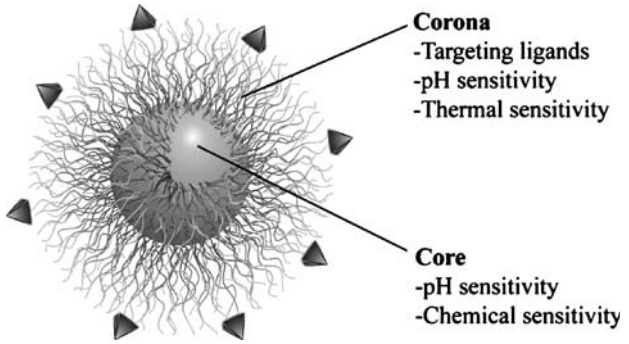

Fig. 2. Schematic diagram of functionalized polymer micelles with active targeting to tumors and responsive drug release properties.

present at the surface of the micelles via X-ray photoelectron spectroscopy (XPS) studies. These folate-encoded micelles were tested against non-malignant human fibroblasts and two cancer cell lines (MCF-7 and HeLa 229 cells). While non-targeted PEG-PCL micelles did not show significant toxicities in all three cell lines (15–22% cell death), the folate-encoded micelles increased toxicity in the two cancer cell lines (44–45% cell death) with folate receptor expression, but not in the normal fibroblasts (20%). Side-by-side comparisons of folate conjugation through hydrophilic PEG vs. hydrophobic PCL terminal ends should provide useful insight on the ligand functionalization strategy.

Micelles functionalized with peptide ligands. Small, tightly binding peptides have also been utilized for cancer-targeted drug delivery. The polypeptide nature of these ligands allows for optimization of ligand behavior via adjustment of the peptide sequence or conformation. One example of this is the cRGD peptide which targets the $\alpha_v\beta_3$ integrin. This integrin is a cellular transmembrane protein that has not only been shown to greatly affect tumor growth, local invasiveness, and metastatic potential, but is also not readily detectable in quiescent vessels (42–44). Moreover, this membrane receptor is highly expressed in angiogenic vessels, making it a target for treating tumors, which are in a constant state of new vasculature growth. Cyclic(Arg-Gly-Asp-D-Phe-Lys) (cRGD) peptides have been developed by Kessler *et al.* to provide specific binding to $\alpha_v\beta_3$ integrins, proving to be 170 times more active than the linear form with an IC_{50} of 8 nM (45–49). Cheresh *et al.* have used ligands targeting the $\alpha_v\beta_3$ integrin to induce complete tumor regression via targeted gene delivery (50). Previous work in our lab has established the formation of cRGD-labeled polymer micelles and micelle targeting to $\alpha_v\beta_3$-overexpresing tumor endothelial cells (SLK cells) (51). Maleimide-terminated poly(ethylene glycol)-poly(ε-caprolactone) (MAL-PEG-PCL) copolymer was synthesized and conjugated to cRGD ligand after micelle formation. Doxorubicin was encapsulated inside the micelle core and its intrinsic fluorescent properties ($\lambda_{ex} = 485$ nm, $\lambda_{em} = 595$ nm) permit for the study of cell uptake by flow cytometry and confocal laser scanning microscopy. Flow cytometry studies show that the percentage of cell uptake increased with increasing cRGD density on the micelle surface. With 5% cRGD surface density, a modest threefold increase of cell uptake was observed, while a more pronounced 30-fold increase was observed by flow cytometry with 76% cRGD attachment. In the presence of excess free RGD ligands, the $\alpha_v\beta_3$-mediated cell uptake can be completely inhibited (51).

Micelles functionalized with carbohydrate ligands. Asialoglycoprotein receptor (ASGPR) is a membrane lectin receptor that is commonly found in liver cells (52). Carbohydrate molecules such as galactose and mannose are found as specific ligands to this receptor (53,54). As it is relatively particular to the liver, ASGPR-based strategies have been used to target drugs for treatment of liver diseases (55). In addition to being present in normal liver cells, ASGPR is also

Table III. Ligand-targeted Micelle Formulations

Ligand Type	Ligand	Polymer Composition	Micelle Size (nm)	Drug	*In Vitro* Model	Animal Model	Ref
Small Organic Molecule	Folic Acid	PEG-PLGA	105	DOX	KB cell	KB in nu/nu mouse	(38)
	Folic Acid	PEG-Dox	200	DOX	KB cell, A549	KB in nu/nu mouse	(39)
	Folic Acid	PEG-PCL	50-130	Paclitaxel	MCF-7, HeLa		(40,41)
Peptide	cRGD peptide	PEG-PCL	20-40	DOX	SLK		(51)
Carbohydrate	Galactose	poly(L-benzyl l-glutamate)-PEG	104	Paclitaxel	P388, SK-Hep 01, HepG2		(57)
	Lactose, Galactose, Mannose, Glucose	PEG-PLA	38–42				(58)
	Galactose	PEG-PLA	32				(59)
	Lactose	PEG-PLA	20–40				(60,61)
Antibody	Anti-GFA Ab	Pluronic	Not reported	Haloperidol		Mouse	(62)
	mAb 2C5 mAb 2G4	PEG-PE	20	Paclitaxel	LLC, EL4 T, BT20	LLC in C57BL/6J mice	(63)
RNA Aptamer	Anti-PSMA aptamer	PEG-PLA	168	Docetaxel	LNCaP	LNCaP in BALB/c mouse	(66,67)

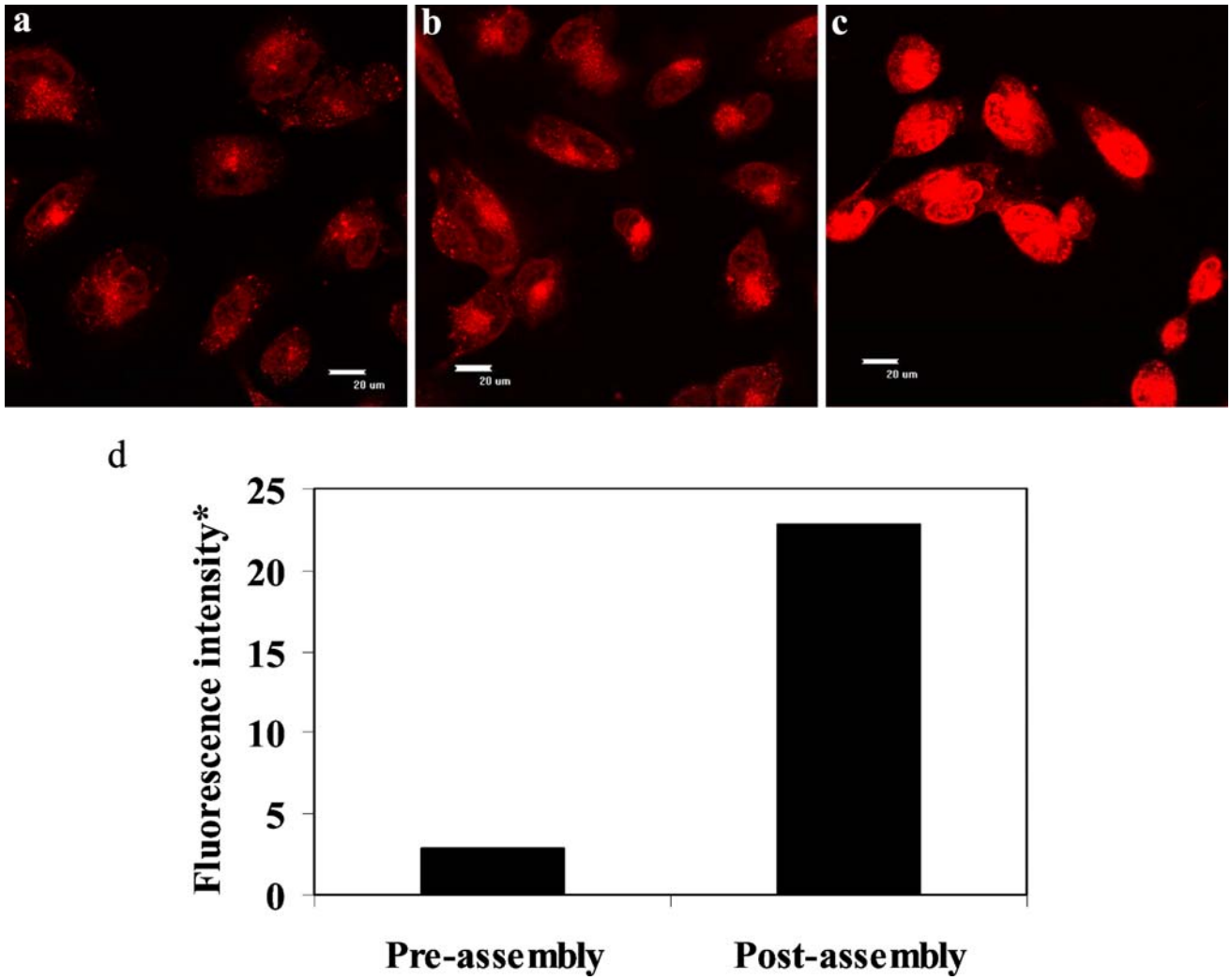

Fig. 3. Confocal laser scanning microscopy of DOX fluorescence of SLK cells after incubation for 1 h with **a** 0%, **b** 50% pre-, and **c** 50% post-micelle ligand attachment, respectively. DOX fluorescent images were obtained with $\lambda_{ex} = 485$ nm, $\lambda_{em} = 595$ nm. The *scale bars* are 20 μm in all three images. **d** Relative mean fluorescence intensity of 50% cRGD-DOX micelle with pre- and post-micelle ligand attachment in SLK tumor endothelial cells as measured by flow cytometry. *Fluorescence intensity corrected for non-targeted DOX-containing micelles.

overexpressed in hepatocellular carcinoma (56), which makes it a useful target for liver-specific chemotherapy. Cho *et al.* synthesized galactose-conjugated poly(ethylene glycol)-co-poly(γ-benzyl L-glutamate) block copolymer (gal-PEG-b-PBLG), and loaded paclitaxel inside the micelles (57). *In vitro* cytotoxicity studies showed that an ASGPR-expressing cancer cell line had greater uptake of these micelles with a 30% increase in cytotoxicity compared to an analogous non-ASGPR expressing cell line SK-Hep01.

Kataoka *et al.* developed carbohydrate-conjugated PEG(4.9 kD)-b-PLA(4.5 kD) micelles and evaluated their binding affinity to a representative cell surface receptor, *ricinus communis* lectin *in vitro* (58–61). First, galactose and glucose were attached to a PEG-PLA copolymer (58). The chemistry is of note since the ligand was used as the initiator from which the PEG-PLA was synthesized through ring-opening polymerization. The high reaction efficiency and low polydispersity of the resulting copolymer allowed for the formation of micelles with up to 90% of the PEG chains functionalized with ligands.

The carbohydrate lactose was also used to produce targeted PEG-PLA micelles (60,61). In this case, a different but equally noteworthy chemistry was used to make the micelles, 3, 3′ diethoxypropanol (DEP) was used to initiate the ring opening polymerizations and the resulting acetal-PEG-PLA was then self-assembled into micelles and incubated at pH 2 whereupon the acetal converts to an aldehyde. The aldehyde end groups on the micelle were then reacted with an amine-containing lactose via Schiff base formation, which was then reduced using NaH_3BCN. This chemistry has the advantage of creating low polydispersity block copolymers while keeping the versatility of allowing any amine-containing ligand to be attached to the micelles. Lectin binding studies of the resulting micelles demonstrated multivalent advantage of micelles over ligand-conjugated small molecules (60,61). As an example, 80% functionalized lactose-encoded micelles were found to bind in a trivalent manner with fast association kinetics ($k_a = 3.2 \times 10^4$ $M^{-1}s^{-1}$) but very slow dissociation constants ($k_d = 1.3 \times 10^{-4}$ s^{-1}). This multivalent effect increased the association constant by over

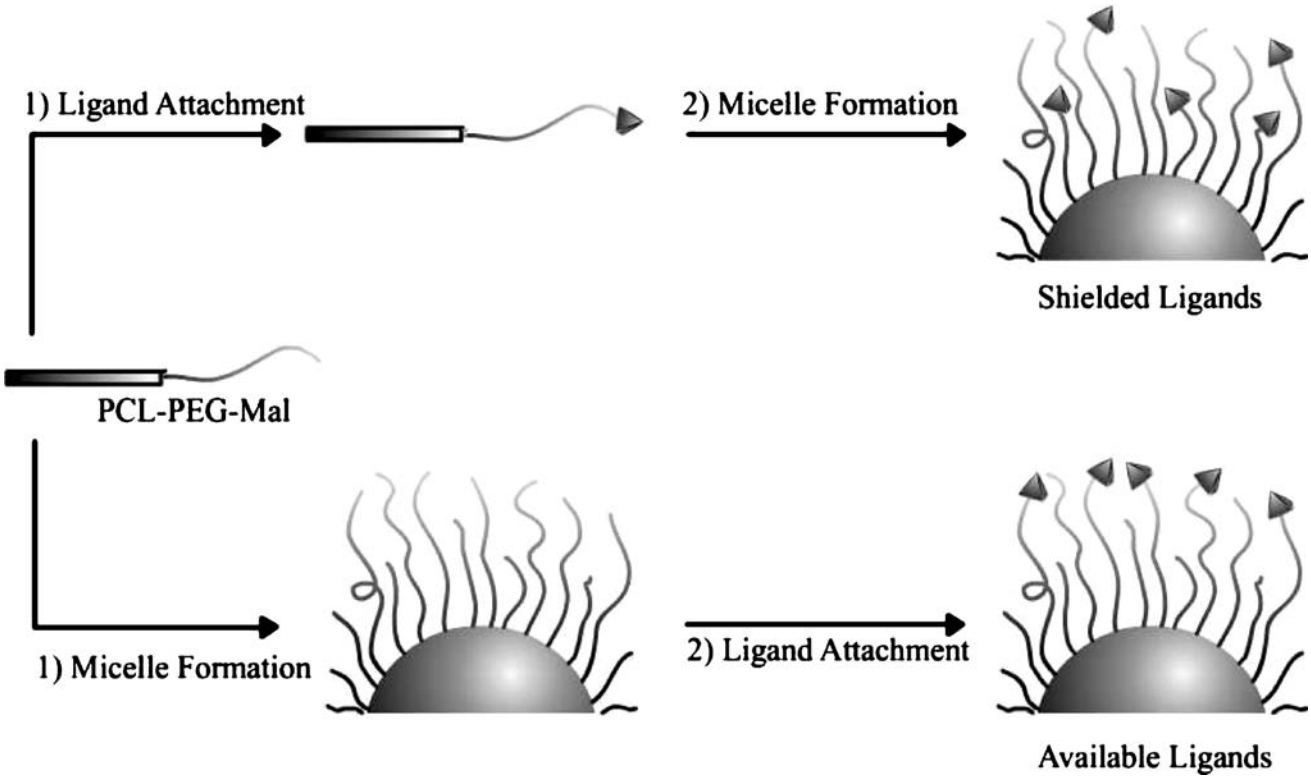

Fig. 4. Scheme showing hypothesized ligand availability through ligand attachment before (*top path*) or after micelle formation (*bottom path*).

twofold while decreasing the main dissociation constant by 145-fold compared to the 20% functionalized micelles, which behaved like monovalent systems. This was attributed to the additional ligands being able to bind to additional surface receptors after initial binding. This additional binding helps micelles to remain attached to receptor covered surfaces and prevents detachment.

Micelles with monoclonal antibodies as targeting ligands. Another promising class of tumor targeting ligand is cancer-specific monoclonal antibodies. These large (~150 kD) and high affinity (Kd ~ 0.1 nM) ligands have the advantage of being able to be customized to bind specifically to a large variety of targets such as cancer cell specific antigens. These were among the first ligands used for micelle targeting, with Kabanov *et al*. using them to target haloperidol loaded pluronic micelles (the major application proposed was for psychiatric treatment). Brain specific antibody conjugation increased the neuroleptic action of the loaded micelles by fivefold over non-targeted micelles and 20-fold over free drug (62).

Torchilin *et al*. developed these ligands to target micelles to lung cancer cells. Diacyllipid-PEG-conjugated polymer (PEG-PE) micelles were functionalized with one of two antibodies, either an anti-cancer monoclonal antibody (mAb 2C5), or an anti-myosin mAb 2G4 (63). Both antibodies retained their ability to bind to their substrates after conjugation to micelles. Moreover, the 2C5 antibody targeted micelle was loaded with paclitaxel and induced a fourfold increase in drug accumulation at the tumor after 2 h, with a corresponding increase in anti-tumor efficacy. Another advantage of the use of antibodies is their high binding affinity that can result in improved behavior with as few as ten antibody ligands per micelle. As high levels of surface modification can lead to unintended non-specific uptake of micelles, it is a great advantage to be able to target micelles with small levels of surface modification. These immunomicelles illustrate this, showing increased tumor accumulation and anti-tumor efficacy but no significant change in blood clearance rate from the non-targeted control samples (63).

Micelles functionalized with aptamers. Aptamers are DNA or RNA oligonucleotides that can be identified from screening a random library to specific molecular targets (64,65). These agents are stable *in vitro*, tumor specific, generally considered non-immunogenic and provide a new targeting platform for micellar drug delivery applications. Farokhzad *et al*. used an RNA aptamer for the prostate-specific membrane antigen (PSMA) to target PEG-PLA micelles to prostate tumors (66,67). These nanoparticles showed specific binding to PSA-expressing cancer cells, with the aptamer inducing a 77-fold increase in binding versus the control group (66), and were subsequently loaded with docetaxel and examined in prostate cancer treatment (67). *In vitro* assays using LNCaP prostate cancer cells demonstrated that aptamer-encoded micelles had a significantly increased cytotoxicity over non-targeted counterparts (the targeted particles showing roughly 50% greater lethality). *In vivo* studies were carried out via intra-tumoral injection of the micelle nanoparticles into LNCaP xenografts in a nude mouse model. The targeted nanoparticles were able to not only show significant increase in anti-tumor efficacy over their non-targeted control, but they were also able to induce total tumor regression in five of the seven mice in the group (in comparison, the non-targeted nanoparticles resulted in only two of the seven mice). In addition, the surviving mice also showed lesser levels of systemic toxicity as determined

by weight loss, than the mice treated with non-targeted counterparts. The presence of DNA or RNA degrading enzymes in the blood may prevent the use of these ligands during intravenous administration, however their initial promise warrants exploration of methodologies (such as development of aptamer analogues) that can increase the *in vivo* stability.

Strategies to optimize ligand presentation. Ligand targeting strategies have had mixed results, with some instances of striking success (38,39,68,69) as well as some with less than successful outcome (70,71). In the latter cases, lack of ligand binding had been attributed to the dynamic nature of the PEG corona which can take on conformations that buries the ligand within the hydrophilic chains (70). Moreover, the polydisperse nature of the PEG chains contributes to this problem as ligands can attach to shorter PEG chains and end up shielded by longer chains. These factors indicate that components within the micelle design can have a negative impact on the binding of attatched targeting ligands to cell surfaces. These considerations have led to a series of studies and micelle designs aimed at optimizing the binding efficiency of the targeted micelles, focusing on methods that minimize the shielding effects of the PEG corona and maximize the chemical availability of the targeting ligand.

Ligand optimization strategies have been explored experimentally by our laboratory. In this case, a single ligand/micelle system was used, but two different strategies were applied for ligand attachment to the micelle. In one case, the cRGD ligand was attached to the PEG-PLA copolymer before micelle self assembly. In the second case, the micelles were assembled first, and the ligand attached afterwards, a method that would ensure that the ligand was attached to chemically available sites on the micelle surface. In both cases, doxorubicin was loaded into the micelles and uptake measured by doxorubicin fluorescence. As shown in Fig. 3, ligand attachment before micelle assembly (Fig. 3b) led to only a modest increase in cellular uptake when compared to a non-targeted micelle control (Fig. 3a). However, cRGD attachment to already formed micelles resulted in a marked increase in uptake (Fig. 3c), suggesting that the alternate ligand attachment route aided ligand availability. Confocal microscopy demonstrated this as well as flow cytometric studies (Fig. 3d). Although the two methods would appear to be similar, they are different upon consideration of the polydisperse nature of the PEG corona. As Fig. 4 illustrates, when the ligands are attatched to the copolymer before micelle formation, they are likely conjugated to the shorter PEG chains within the population and suffer from shielding effects (Fig. 4, top path). This may be worsened by higher chemical reactivity of shorter polymer chains, which induces an additional selection pressure for ligands to be tethered to the short chains. There is also the possibility that some hydrophobic ligands may have aggregated inside the micelle core rather than being presented at the surface. In contrast, the post-micelle ligand addition strategy would select for ligands attaching to longer PEG chains which aids in ligand presentation for subsequent binding to cell surfaces (Fig. 4, bottom path).

Computer modeling has also been used to investigate ways to optimize ligand presentation to improve targeting. Chen and Dormidontova explored ligand valency and bidisperse PEG layers as methods to increase ligand presentation (72) (Fig. 5). As cells are very large (~10 μm in diameter) in comparison to micelles (10–100 nm), the cell surface was modeled as a flat plane and the micelle corona modeled as a polymer brush with surface binding ligands on the chain ends. In this case, it was found that multivalency did aid in binding ability, but only when the receptors were closely packed on the cell surface. This can also be used to aid in ligand choice, as some ligand receptors, such as the $\alpha_v\beta_3$ integrin, are known to cluster together upon binding (73), bringing the receptors closer together and aiding in the efficacy of multivalent ligands. Moreover, use of a bidisperse corona design where the ligand is conjugated on the terminal end of longer PEG chains but the corona is composed of shorter PEG chains, also leads to a theoretically increased

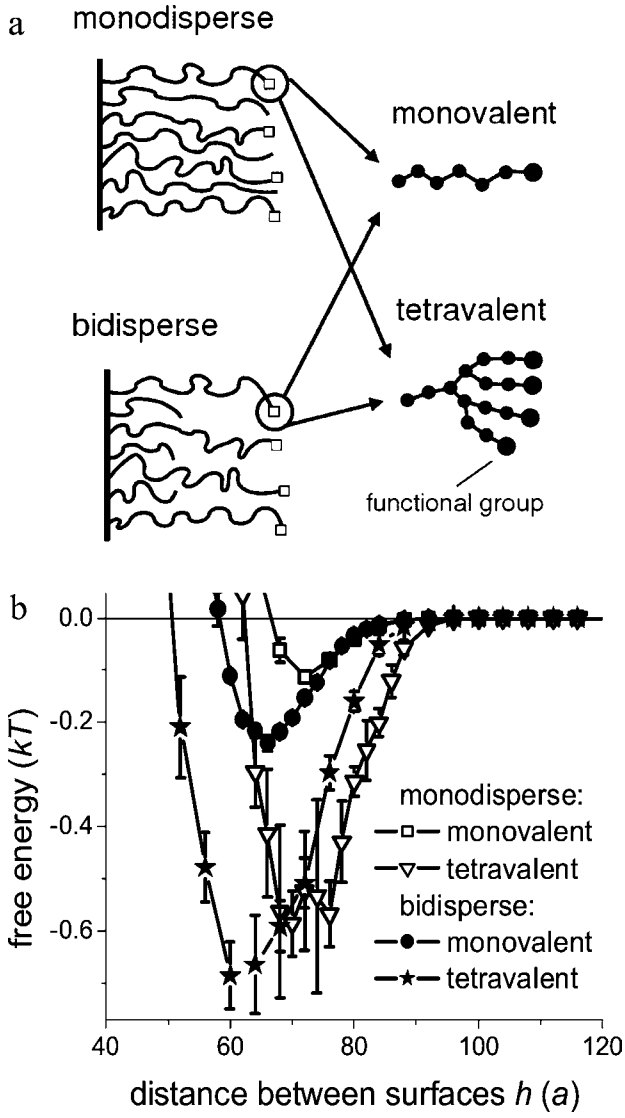

Fig. 5. **a** Schematic describing the tetravalent/monovalent ligand design and bidisperse PEG corona layers to enhance ligand presentation. See reference (72) for more details. **b** Free energy diagram describing the binding energy profile for the ligand/corona types (72).

Table IV. Micelle Formulations that Allow for Site-specific Drug Release

Polymer Composition	Release Mechanism	Size (nm)	Drug	Cancer Cell Line	Animal Model	Ref
pH Sensitivity						
Acid Labile Bonds (Covalent)						
PEG-PLA-DOX	Acid Labile Bond	89	DOX	HSB-2		(75)
PEG-p(Asp-Hyd-DOX)	Acid Labile Bond	65	DOX	SBC-3, KB cells, C26	Mouse	(76–78)
PEG-Acetal Linked Dendritic Polyster/ Polylysine	Acid Labile Bond	35	Nile red, DOX	MDA-MB-231		(79–81)
Non-covalent pH Sensitivity						
Hydrophobic Core						
Cationic Porphyrin Dendrimer, PEG-pAsp	Charge Neutralization	55	Porphyrin dendrimer	LLC		(82–83)
PEG-DMA-DEA	Amine protonation	30–50	Dipyridamloe			(84)
PLA-PEG PHis-PEG	Histidine protonation	50–114	DOX	MCF-7	BALB Mice	(85,87,88)
Pluronic+ β-amino ester	Beta amino ester protonation	130	Paclitaxel	BT-20, MDA-MB-231	Nu/Nu Mice	(90–92)
pNIPAM Coplymer	Protonation of Undecanoate	160–200	DOX			(93)
pNIPAM coplymer	Protonation of Undecanoate	35	AlClPc	EMT-6		(94–96,129)
Hydrophillic Core						
PEG-EAMA	Nanogel Swelling	49–681				(97)
PEG-PMA	Nanogel Swelling	130	Cisplatin			(98)
Temperature Sensitivity						
PNIPAM-	LCST Transition	12–31	DOX	Bovine Aorta Endothelial		(23)
PNIPAM-PLA	LCST transition	40–65	DOX	Bovine Aorta Endothelial		(105)
PNIPAM-PBMA	LCST Transition	338	DOX	Bovine Aorta Endothelial		(24)
PNIPAM-copol-PLGA	LCST Transition	85–120	Paclitaxel	MDA-MB-435S		(103,105,107)
Cholesterol Endcapped Acrylamides	LCST Transition	100–200	Pyrene			(103)
Ultrasound Activation						
Pluronic, PEG-lipid	Ultrasound	12.9	DOX, Ruboxyl	HL-60, A2780, A2780/ADR, MCF-7	Nu/Nu mice	(115–120)
NNDEA Pluronic	Ultrasound	50–100	DOX	HL-60, DHD/ K12/TRb	BDIX Rat	(121–124)
Enzyme Response						
PEG-Peptide pNIPAM	Phosphorylation	50–100				(125)
Oxidation						
PEG-Polysulphide	Sulphide Oxidation	75				(126)

binding affinity (as calculated via free energy minimum in Fig. 5b). In this case, the shorter PEG chains provide a steric barrier preventing the ligand from curling back into the micelle corona layer.

The use of ligand targeting strategies in micelles has enabled the development of site-specific nanodevices with improved uptake and efficacy. Advances in the understanding of tumorigenesis have led to the discovery of a growing number of unique surface markers whose expression differentiates tumor from normal tissue and provides a means of achieving active targeting to tumors. This variety of ligands allows for the customization of micelles to a diverse number of cancer types.

SITE-SPECIFIC DRUG RELEASE

Drug encapsulation inside polymer micelles will considerably alter drug pharmacokinetics leading to an increase in drug targeting to tumor tissues. After reaching the targeted site, efficient drug release from micelle carriers becomes critically important to ensure drug bioavailability, and hence achieve the desired cytotoxic effect. In the section below, we review the various engineering strategies concerning the tailoring of micelle structures to trigger drug release at the tumor site. Table IV provides an overview of micelles designed for site-specific drug release.

pH sensitive drug release. Despite the general impression that the body has a uniform pH of 7.4, intravenously

administered nanodevices can encounter several instances of pH change that can facilitate drug delivery. Firstly, tumors tend to have lower pH values (as low as 5.7) than normal tissue environment (pH 7.4) (74). This acidification is due to the general characteristic of cancer cells to rely on glycolysis for metabolism. Changes in pH are also encountered once nanodevices enter cells via endocytosis. Endocytosis is the sequestration of the nanocarriers into an early endosome, which is accompanied by an increase of acidity inside the vesicle as it matures into late endosomes and heavily degradative lysosomes (pH 5.0–5.5). Both the acidic nature of tumor tissue and endocytosis provide ample applications for pH responsive micelles which release their contents upon exposure to acidic environments. Two strategies are generally used to induce pH sensitivity into a micellar system. The first is a covalent strategy involving the use of acid-labile bonds, while the second is a non-covalent strategy involving the selective protonation of pH-sensitive components inside the micelle.

Acid-labile bonds. pH sensitivity can arise from the creation of an acid labile linkage between the drug and the polymer forming the micelle (75–78). Covalent modification of the polymer with the drug allows for extremely high loading since the drug is itself an integral part of the micelle rather than merely an encapsulated agent during micelle formation. However, the main disadvantage of this method is the requirement of functional groups on the drug molecule that can be covalently modified, and since not all drugs are capable of being conjugated to a polymer in such a way, the scope of this method is limited. The most effective uses of acid labile bonds have been the direct conjugation of doxorubicin to the hydrophobic portion of a micelle forming block copolymer. Initially this was demonstrated by Park et al., who used either a hydrazone or *cis*-acotinyl bond to link doxorubicin to the PLA end of PEG-PLA micelles (75). Although the *cis*-acotinyl linkage has a greater level of pH sensitivity in drug release with a roughly tenfold increase in release rate at pH 5.0 over 7.4, the *cis*-acotinyl linkage results in the release of a chemically modified drug whereas the hydrazone linkage, with a roughly fourfold increase in release rate, degrades cleanly and releases unmodified drug. The hydrazone linked micelles also have a fivefold greater cytotoxicity than free drug, given that endocytosis leads to greater uptake in the micellar DOX than passive diffusion does of the free drug. Though the PEG-PLA end modification in this case leads to favorable results, drug conjugation solely on the end group leads to a functional micelle with a relatively low loading (3.7%).

Kataoka *et al.* took a different approach and conjugated the drug to the aspartic acid residues of a polyethylene glycol poly (aspartic acid) (PEG-pAsp) copolymer via a hydrazone linkage (76–78). Though the precursor block copolymer is fully hydrophilic, the bonding of doxorubicin to the aspartic acid residues induces hydrophobicity in the pAsp segments. The resulting micelles achieved a DOX loading content as high as 42.5%; to date the highest drug loading content reported in a micelle of this size (less than 100 nm). These micelles had almost no release of drug at pH 7.4 (less than 3% after 48 h) but released drug in solutions of pH 5.5 with 25% of the drug released after 48 h. Near complete release of drug was observed at pH 3.0, with HPLC analysis demonstrating release of functional drug. Though these micelles have less *in vitro* cytotoxicity than unconjugated drug (the IC_{50} of micelles being tenfold that of DOX), it was demonstrated via fluorescence microscopy that the micelles were indeed taken up by the cells after 3 h of exposure and drug released to the nucleus. *In vivo* studies demonstrated the utility of this micellar system. Biodistribution studies showed that while only 2% of free drug deposits in the tumor, micellar encapsulated drug improves this value to 10%. This additional tumor deposition was accompanied by a great increase in the tolerance for drug (15 mg/kg for free drug, compared to 40 mg/kg for micelle encapsulated drug). The micelles were then able to not only demonstrate greater tumor growth inhibition in mice, as well as induce complete tumor regression in 50% of the mice tested, outperforming the highest tolerated doxorubicin dose which only resulted in a complete cure in 17% of the mice (78).

Acid-labile bonds have also been used as a structural component of the micelle polymer backbone (79–81). In this way, the micelle itself can degrade as a function of pH resulting in a micelle that should be pH sensitive regardless of the drug used. These micelles are designed to release drugs as a result of acid catalyzed polymer degradation. Frechet and co-workers achieved this in a micellar system using hydrophobic groups attached to the hydrophobic dendrimer ends of a PEG-dendritic polylysine or PEG-dendritic polyester copolymer. These terminal hydrophobic trimethoxy benzyl groups were linked to the dendrimer via acid-sensitive acetal linkages. These unusual copolymers self-assembled into small micellar nanoparticles of between 20 and 50 nm with cores designed to degrade via acid catalyzed hydrolysis. Hydrolysis of the structures could be directly followed by UV/Vis spectrometry due to trimethoxybenzaldehyde residues that are released from the micelles upon degradation. The acetal group is easily hydrolyzed under acidic conditions and the resulting micelles show pH dependent degradation that is alterable via the change of the characteristics of the non-acetal portion of the hydrophobic dendrimer, with more hydrophilic cores degrading more quickly than more hydrophobic ones. In most cases, the amount of degradation seen at pH 7.4 was negligible (less than 5%) after 24 h, but high levels of degradation (80–100%) could be observed under pH 5.0 conditions for the same time period (79,81). In order to explore the use of this system for drug delivery, doxorubicin was loaded into these micelles. The DOX loaded micelles showed favorable size and loading (35 nm, 12% loading) and excellent pH sensitivity in their release, with a tenfold increase in release rate at pH 5.0 over pH 7.4. In order to account for innate DOX pH sensitivity, controls were performed by releasing DOX from a comparable non-pH responsive micellar assembly which showed only a twofold increase in release at acidic pH.

Non-covalent strategies. The other commonly used method to achieve pH sensitivity is a non-covalent strategy whereupon an ionizable component within the micelle structure alters conformation upon protonation. As an example, Kataoka *et al.* used charge–charge interactions to build a micelle core carrying a positively charged zinc porphyrin dendrimer. The core of the micelle in this case is composed of a positively charged porphyrin dendrimer which

has been neutralized by the negatively charged residues of a PEG-poly(L-aspartic acid) copolymer. This micelle is stable at neutral pH, but at pH above 8 or below 6, these micelles destabilize due to loss of charge balance in their core. This pH dependent stability results in a system which will remain stable until it is taken up by cells, whereupon the micelle will degrade after cellular uptake. These spherical 55 nm particles demonstrated roughly one third the uptake of non-encapsulated photosensitizer due to charge neutralization of the porphyrin preventing charge–charge interactions of the positively charged porphyrin with negatively charged cell membranes. While the uptake of the porphyrin was impeded by micelle encapsulation, the photodynamic efficiency of the micelles was 40 times higher than that of free porphyrin, a result of the micelle preventing porphyrin aggregation (82,83).

Whereas the above system uses a polyanion in the micelle, it is more common to build pH responsive micelles based on hydrophobic polycationic systems. Tang *et al.* designed a triblock polymer of PEG, poly (2-(dimethylamino) ethyl methacrylate) (DMA), and poly(2-diethylamino)ethyl acrylate (DEA) resulting in a system that dissolves completely in acidic solution but forms micelles at high pH (pH 8.0). Pyrene exclusion studies demonstrated that these micelles reversibly form at pH 7.0 and above, and break apart when the pH is less than 6.0. This group used the acid sensitivity of this copolymer alongside an acid sensitive model drug (dipyridamole) to make a high loading micelle (19%) without a requirement for organic solvent. Acid sensitive release of the agent was observed with a 50% increase of drug release at pH 3.0 over that at pH 7.4 (84).

Bae *et al.* used a block copolymer of polyethyelene glycol and poly(L-histidine) (PEG-pHis) to fabricate pH sensitive micelles (85–88), where the histidine residues are hydrophobic at neutral pH (histidine has a pKa of 6.1) but protonate at the endosomal pH (5.5), resulting in a buffering effect that can induce micelle destabilization (85,87,88). Titration studies confirmed that the polyhistidine residues retained their buffering capacity within the physiologically relevant range between pH 8.0 and 6.0. Variable protonation of the histidine residues resulted in a copolymer whose CMC was tenfold greater at pH 5.0 than 7.4. Pyrene exclusion assays and light transmittance studies both confirmed that the micelles underwent dissociation when suspended in buffers with pH below 7.4. PEG-pHis micelles are unstable at pH 7.4 (85), but inclusion of a more stable PEG-PLA component to the micelle formulation resulted in micelles stable enough for clinical use (88). The inclusion of the second component also brings the activation pH to between 6.6 and 7.2, making these micelles viable for tumor targeting via pH changes. These micelles were further functionalized with folate targeting ligands and are more comprehensively discussed in the section on 'multifunctional micelles.'

Recently, the pH dependent solubility of poly(β-amino ester) (89) has been established for the creation of pH-sensitive micelles (90–92). These biodegradable polymers are hydrophobic at neutral pH but can become fully soluble at pH below 6.1. This pH dependent solubility can lead to almost instantaneous release of their contents from microparticles upon acidification (89). Amiji *et al.* used a strategy of surrounding a hydrophobic poly(β-amino ester) core with a PEG corona from the pluronic copolymer F108 (90–92) in order to fabricate nanoparticles. These resulting micellar nanoparticles were loaded with paclitaxel (90) and found to form particles between 100 and 150 nm in diameter with loading content of 1% but a remarkable loading efficiency of 97%. *In vitro* microscopy studies using FITC encapsulated particles were used to demonstrate intracellular release. The pH sensitive particles showed release of FITC into the cytoplasm of the cells while a non-pH sensitive FITC nanoparticles control showed punctate fluorescence indicative of no release (91). *In vivo* studies demonstrated that the pluronic modified β-amino ester nanoparticles shared the long residence times and improved half-life that is seen in similar nanoparticles, but shows improved drug deposition in the tumor over not only free drug (23-fold improvement) but also over non-pH sensitive pluronic PCL nanoparticles (threefold improvement) (92).

To a lesser extent, poly(N-isopropylacrylamide) (pNIPAM) has been used in the design of pH sensitive micellar systems. Although pNIPAM is most known for its lower critical solution temperature (LCST) behavior in water, the temperature of the LCST can be adjusted by the incorporation of hydrophobic groups and titratable moieties such as undecanoic acid (93) or methacrylic acid (94–96) to the backbone. In the undecanoic acid case, copolymerization into a poly(N-isopropylacrylamide) backbone in order to act as a titratable group results in a temperature sensitive polymer becoming pH sensitive one. At physiological pH (7.4), the acid is deprotonated and the resulting polymer has a higher than body temperature LCST (38°C), however at lower pH (4,5), the acid becomes neutral and lowers the LCST (29°C). The resulting polymer can have an LCST above 37°C which will shift below this point in response to pH. As a result, it is believed that these polymers will become hydrophobic inside the endosome and disrupt the endosomal vesicle in the cell. Polymer micelles containing DOX were fabricated and a threefold increase of DOX release was observed upon a very sharp pH change of 6.6 over 7.4.

More extensive exploration has been done using pNIPAM with methacrylic acid and octadecylacrylate as the titratable moieties (94–96). This strategy allowed for the customization of the polymer solubility to be water insoluble above pH 6.0, but to solubilize completely at pH below 5.5. Despite the random copolymer structure, these polymers were able to form small nanoparticles of 35 nm. The small size, lack of surfactant required in creation, and critical aggregation concentration suggest micellar characteristics, such as a hydrophilic corona preventing aggregation, leading to the conclusion that these nanoparticles are indeed micelles. The photosensitizer aluminum chloride phthalocyanine (AlClPc) was incorporated into these micelles for applications involving photodynamic therapy against tumors. *In vitro* studies demonstrated the efficacy of this encapsulated photosensitizer against EMT-6 mouse mammary cells with the micelles showing no toxicity unless exposed to light, after which the LD_{90} was found to be 6 μm after 24 h of light exposure (94). Subsequent studies demonstrated these molecules were effective *in vivo* in EMT-6 flank tumors, with the micellar formulation providing complete tumor regression observed at a dose of 0.25 μmol/kg (95).

Hydrophilic core micellar systems have also been developed for the purpose of pH sensitive drug release.

These systems function by creating a cross-linked hydrophilic core which swells and contracts in response to pH much like a hydrogel. Hayashi *et al*. used emulsion polymerization of a PEG-vinyl benzene with 2-(diethylamino)ethyl methacrylate using a diacrylate as a crosslinker to design such a system (97). These nanogels could be as small as 49.5 nm but swelled to over double their previous size within a very small and biologically relevant pH range (7.4–6.0). Kabanov's group used a similar strategy in his crosslinked PEG-poly(methacrylic acid) micelles (98). First calcium was used to induce micellization followed by crosslinking with a diamine. These micelles swelled under basic conditions as the acidic residues would deprotonate and a negative charge would build up within the micelle core, almost doubling the micellar size from 170 to 290 nm. Cisplatin could also be loaded into these cross-linked micelles with a 55% loading efficiency. And while the nanogel strategy for cancer targeted micelles is currently in its infancy, the large pH induced size variations suggest this strategy has a bright future.

Temperature sensitive drug release. The ability to raise local temperatures inside the body makes temperature triggered drug release a viable strategy in site-specific drug release (99). Additionally, tumors have been shown to be more vulnerable to hyperthermia than normal tissue as a result of their chaotic vasculature (99). These two factors give temperature sensitive nanosystems the capability of providing a synergistic therapy, whereupon the elevated temperature not only causes local drug release but also serves to inflict additional damage to tumor cells. Elevated temperatures have also been proposed as a way to induce micellar aggregation at the tumor site, improving biodistribution of the administered agent. In the case of the creation of temperature sensitive micelles, the most common technique is the use of an LCST behavior polymer as the corona of the micelle (23,24,100–104). The most extensively used polymer for this purpose is Poly(N-isopropylacrylamide), or pNIPAM. Pure pNIPAM homopolymer has an LCST of 32°C which can be adjusted by random copolymerization with monomers such as dimethylacrylamide in order to obtain LCST values within a desired range. The resulting micelles are stable below the LCST, but temperature increase above the LCST induces the entire system to be hydrophobic and precipitate out of solution.

Okano *et al*. initially used polystyrene (PS) to form the hydrophobic core while pNIPAM was used for the thermosensitive corona (23). The resulting micelles had a transition temperature of 32°C and did indeed show reversible aggregation behavior as shown by optical transmittance. Unfortunately, they did not show temperature-triggered drug release. An alternative was later found by this group in a hydrophobic core of poly(D,L-Lactide) (105). The pNIPAM/PLA micelles also showed reversible aggregation behavior, but again had a transition temperature that was too low for immediate *in vivo* use (32°C). This group developed a temperature responsive release system by using a low Tg hydrophobic polymer such as poly(butyl methacrylate) (PBMA) (24) as the core-forming segment. pNIPAM-bPBMA micelles showed reversible aggregation at a transition temperature of 34°C, and could be loaded with doxorubicin with a pronounced temperature release sensitivity, only 15% of the drug was released after 15 h at 30°C, as compared to a temperature to 37°C, where 90% drug release in the same time period. The release could also be conditionally switched on and off using temperature cycling. Additionally, these micelles demonstrated temperature sensitive cytotoxicity, since the loaded micelles showed almost no toxicity at a 0.1 μg/ml dose at 29°C (less than 5% cell death) but greatly increased toxicity when the temperature was increased to 37°C (65% cell death). In order to determine the mechanism for release, fluorescent probes were incorporated into these micelles, revealing alterations in the core micropolarity upon heating despite the fact that the core itself is not thermoresponsive. It was proposed that a low Tg polymer core (PBMA has a Tg of 20°C) is more subject to core deformation than a high Tg core upon temperature transition of the corona forming polymer. Side-by-side comparisons with an analogous system using a high Tg core (polystyrene core, Tg = 105°C) confirmed this hypothesis, as the higher Tg core micelles were designed to have the same LCST corona behavior as the lower Tg system, but showed little or no temperature dependent cytotoxicity or drug release (106). This group refined the design further by incorporating hydrophobic dimethylacrylamide (DMA) into the pNIPAM segment in order to raise the LCST temperature (105,107). These resulting systems were able to show biologically relevant transition temperatures as high as 42.5°C. The core polymer used, in this case, was PDLA, chosen for its low Tg (35°C). The DOX loaded pNIPAM-coDMA-bPDLA micelles was sufficiently mobile for temperature sensitive doxorubicin release (4–5-fold faster release at 42.5°C over 37°C), and temperature sensitive cytotoxicity was retained despite the higher Tg core.

pNIPAM/PLGA micelles have also been reported (93,108) by Yang *et al*. In this case, pNIPAM copolymerization with dimethylacrylamide (DMMAAm) resulted in materials with a desirable LCST of 39°C. The low Tg core of these micelles was also able to be sufficiently deform for temperature sensitive drug release, in particular when the PLGA segment length was short when compared to the hydrophilic region. This demonstrates a balance that must be considered when designing these systems, for longer hydrophobic segments appear to result in larger drug loading contents but a lesser intensity of temperature sensitivity to the release kinetics. In this case, paclitaxel was loaded in the micelles, rather than DOX. The more hydrophobic nature of paclitaxel allowed for very high loading (20%) and functional loading efficiency (50%). Fine tuning of the temperature sensitive and hydrophobic segment lengths allowed for the creation of a system which showed temperature sensitivity over a very tight range, with a fourfold increase in paclitaxel release and eightfold increase in cytotoxicity at 39.5°C over those at 37°C.

Other methods have been used to adjust the LCST behavior of pNIPAM. Hydrophobic grafting and end capping also results in polymers capable of temperature sensitive micellar systems (103). These systems tend to produce larger micellar particles than block copolymer strategies, but manipulation of the LCST behavior of the materials simply consists of adjusting graft density or copolymer content. Liu *et al*. attached cholesterol onto a pNIPAM copolymer in this fashion, resulting in an amphiphillic polymer capable for forming micellar constructs and encapsulating drug (103). Cholesterol end-capping resulted in a polymer with an LCST too low for use *in vivo* (33°C), but the grafting strategy

resulted in a material with LCST in the desirable range of slightly above body temperature (38°C). In spite of this, temperature increase only induced a roughly 50% increase in drug release, possibly due to the inability of the pNIPAM transition to sufficiently deform the micelle core.

Ultrasound-triggered drug release. Ultrasound is used in medicine for diagnostic and therapeutic applications and has proven to be a non-invasive method to access and treat many problems including strokes, osteoporosis, and cardiovascular disease (109). This method is also currently being explored as a trigger for drug release for either implanted drug depots (110) or injected nanodevices such as liposomes (111). The complexity of interactions of tissue with ultrasound gives insight as to the utility of this method for drug delivery. The most immediate effect is the local increase in temperature of the exposed tissue as a result of ultrasound waves which was shown to be sufficient to induce drug release in appropriately designed micelles. Cavitation also occurs, where small oscillating bubbles are rapidly produced and collapsed. This exposure has been shown to induce shear forces on tissue and has many effects including increasing the permeability of the cell membrane (112) and increasing the uptake of gene delivery vectors (109). Finally, ultrasound treatment produces small amounts of highly reactive free radical species which could possibly serve as a chemical trigger to an ably designed system.

To date, the most extensive exploration of ultrasound triggered drug release in polymer micelles has been done with pluronic micelles. As mentioned previously, pluronic is a ternary copolymer of PEG and PPO that has been shown to have little cytotoxicity and has been used for many biological applications including as a bioadhesive, hydrogel matrix (113), and in gene delivery (7). The polymer also appears to have a synergistic effect with some chemotherapeutic agents and has been proposed to inhibit the p-glycoprotein that causes multidrug resistance in many cancer cells (114). Pitt *et al*. explored ultrasound as a means to induce drug release of doxorubicin from pluronic micelles (115,119). Even without ultrasound, pluronic has a synergistic effect with the doxorubicin, increasing the toxicity of the chemotherapeutic agent twofold in spite of decreased uptake of the doxorubicin into the cells. Ultrasound treatment further increased the toxicity of the drug containing micelles another sixfold (118). In order to explain this, it was proposed that the presence of pluronic unimers aided the toxicity of the drug (119) but the micelles actually sequestered drug away from the cells until ultrasound induced drug release (115,119). The presence of sequestered drug inside the hydrophobic core was determined fluorescently using a doxorubicin analogue, ruboxyl, and it was found that up to 70% of the ruboxyl was sequestered inside of the micelles (118). This hypothesis was further confirmed upon exploration of DNA damage to the treated cells, where micelle encapsulated doxorubicin did not show detectable DNA damage (via Comet assay) unless ultrasound was applied. Flow cytometric exploration suggested that ultrasound also increased the permeability of the cell membrane as well as induced DOX release from the micelles (119). The frequency of ultrasound was also found to affect drug release from pluronic micelles, with an increase of the ultrasound frequency from 67 kHz to 1 MHz lessening the degree of drug release from the micelles by threefold. Despite the decrease in drug release, the increased frequency did increase cell uptake, suggesting that the ultrasound increased cell permeability.

Pluronic micelles have the disadvantage of being less stable upon dilution than most other polymer micelle systems, with micelle degradation being reported upon injection (120). As a result, this group incorporated a PEG-phospholipid (PEG-DSPE) making a mixed, stabilized micelle for use in animal studies (120). This system was used in extensive *in vivo* tests exploring anti-tumor efficacy and flow-cytometric biodistribution studies. In these studies, micelles were administered to mice followed by removal of the organs and flow cytometric characterization of the DOX uptake within the tissues. Ultrasound was found to improve the anti-tumor efficacy of both free DOX and micelle incorporated DOX. In the latter case, the ultrasound was able to delay tumor growth an additional 2.6 days over micelles without ultrasound. The biodistribution studies also demonstrated advantages to ultrasound mediated release, with application of ultrasound not only increasing the level of drug accumulation in the tumor (as measured by flow cytometry of recovered tissue), but also lowering the level of drug accumulation in the kidneys. This lower level of kidney exposure, as compared to tumor exposure, was attributed to released drug being eliminated by the kidney rather than micelles, which could be retained. Heart exposure was also lessened, an important result as cardiotoxicity is a major side-effect of traditional doxorubicin administration. In this study, DOX loaded PEG-pAsp(Z) micelles were also studied, and found to convey the same levels of biodistribution improvement as the stabilized pluronics.

Another way to stabilize pluronic micelles is to use an interpenetrating poly(diethylacrylamide) (NNDEA) network inside the micelle core (121–124). These plurogel micelles are equally able to encapsulate doxorubicin, release it upon ultrasonic stimulation, and show the same synergistic effects with drug toxicity as unstabilized pluronics. The plurogels are, however, much more stable upon dilution, with a half-life of roughly 17 h whereas unstabilized micelles rupture almost immediately upon dilution (122). The ability to remain stable upon dissolution allowed these micelles to be used *in vivo* with success. A mouse animal model was implanted with two tumors and given these core-stabilized pluronic micelles loaded with doxorubicin. One of the tumors was sonicated while the other was not and it was demonstrated that the sonicated tumors showed greater response to the chemotherapeutic treatment (124). It is difficult to determine the exact mechanism by which the ultrasound aided the pluronic micelles *in vivo*. The improvement can be due to increased release of the drug at the site, improved extravasation of the micelles as a result of ultrasound exposure to the angiogenic vessels, or a complex interplay of the two effects.

Drug release due to chemical sensitivity. Attempts have been made in micellar systems that respond to more specialized chemical stimulus than pH, temperature, or ultrasound. Although these are in the minority of the functionalized micelle research, they are worth noting.

An enzyme responsive system was designed based on a polypeptide that is a substrate of protein kinase A (125). This polypeptide was linked to pNIPAM and PEG moieties resulting in a micelle-forming polymer at 36°C. These micelles

had a core of pNIPAM and peptide with a PEG corona. Upon exposure to the protein kinase, the peptide portion of the micelle became phosphorylated and hydrophilic, driving the LCST to 40°C, and disintegrating from 200 nm particles to 100 nm, with a corresponding change of the aggregate mass of the nanoparticles from 10 to 2 million Daltons. This is the first report of an attempt at a protein kinase responsive micelle system.

Hydrogen peroxide (H_2O_2) and superoxide radicals are reactive oxygen species that are present in many cancer cells. One system sought to use these as a trigger for a responsive system by creating large polymer vesicles that collapse into smaller micelles upon H_2O_2 exposure (126). These vesicles were based on polymers with a poly(propylene sulphide) hydrophobic segment and a PEG hydrophilic segment. Presence of H_2O_2 oxidizes the sulphide residues into more hydrophilic sulphoxide residues disrupting the vesicles (200–500 nm) that result in formation of much smaller wormlike micelles (~20 nm), the structures and sizes of which were observed via TEM. These nanosystems required an unusually high H_2O_2 concentration (3%) for this conversion to happen, but this method of micelle stimulus shows promise and may yet prove to be more applicable once it has become more finely tuned.

Multi-functional micellar systems. The newest generation of cancer-targeted polymer micelles is based on systems with multiple functionalities. The architecture of a micelle with distinguishable surface, corona, and core allows for the customization of each region to provide functionality. These novel systems use the synergy of receptor mediated endocytosis and pH sensitivity to result in systems that both show enhanced tumor targeting as well as enhanced intracellular drug bioavailability.

Kataoka's group used folic acid to enhance their previous PEG-p(Asp-Hyd-Dox) micelles. As mentioned earlier, the untargeted formulation does show anti-tumor efficacy, but the micelle formulation appears to lessen the cytotoxicity of the encapsulated DOX. The folic acid ligand was linked to the micelle surface in order to selectively increase the uptake of the micelles, increasing their cytotoxicity while retaining low toxicity to non-folate receptor expressing tissues. Ligand targeting improved the cytotoxicity of the micelles, roughly doubling the toxicity of the micelles to KB cells after a 3 h exposure. Given a 24 h exposure, the targeted micelles showed to be equally as cytotoxic as free DOX and tenfold more cytotoxic than the untargeted formulation. Flow cytometry confirmed that the enhanced toxicity is a result of increased uptake of the ligand targeted micelles (77).

Bae *et al*. expanded on their PEG-pHis pH sensitive system (85,87,88) by adding ligand targeting function. Folic acid was conjugated to the pH sensitive micelles resulting in a multi-functional system which incorporated both ligand targeting for enhanced cell uptake and pH sensitivity for enhanced intracellular release. This system performed well *in vitro*, showing equal cytotoxicity as free DOX against MCF-7 cells (88). Further studies on multi-drug resistant MCF-7 cells showed this system to be more than 90% cytotoxic at a concentration of 10 μg/ml while free DOX shows only 10% cytotoxicity (87). This overcoming of the MDR phenotype may have resulted from the alteration of the mechanism of DOX uptake, with the folate targeted micelles being taken up via receptor mediated endocytosis, as opposed to free drug passively diffusing across the membrane. The authors hypothesized that folate mediated receptor endocytosis may overcome the multi-drug efflux pumps. The *in vivo* efficacy was evaluated in mice bearing normal MCF-7 and drug resistant MCF-7 xenografts, with the pH sensitive folate-DOX-micelles showing a 3.6–4.5-fold and a 2.7-fold lesser tumor growth than free drug administration, respectively. Biodistribution studies also showed a much longer circulation time of DOX in blood for both folate and folate-free micelles compared to free DOX. Tumor distribution studies showed that folate-micelles allowed for 20 times more accumulation of DOX in solid tumors than free DOX and three times more than folate-free micelles, which correlates with the improved tumor efficacy with folate-micelles.

Bae *et al*. have also added a previously unsuggested aspect of pH sensitive ligand presentation to the above system. In this case, the targeting ligand was linked to a short block of histidine residues. At neutral pH, the hydrophobic histidine chain draws the ligand near the core of the micelle. Upon acidification, the protonated histidine chain brings the ligand out to the corona where it can be presented to receptor sites (86). These micelles showed pH sensitive cell uptake over a narrow pH change from 7.2 to 7.0, with a tenfold increase in cell uptake at pH 7.0 over that at 7.2. This functionality results in a micellar system that could travel though the bloodstream, specifically present its binding ligands to cells in acidic tumor environments, undergo receptor mediated endocytosis, selectively release drug inside the cell, while preventing non-specific uptake.

Torchilin *et al*. also designed a pH-controlled targeted micelle system via a multidisperse pH sensitive corona design (127). In this system, two targeting ligands are employed on PEG-phospholipid micelles. The first is an antibody attached to the end of a long PEG chain (Mw 3400). The second is a secondary targeting ligand, such as TAT peptide, which is attached to the micelle core via short PEG chains (Mw 2000). The majority of the corona, in this case, is composed of intermediate length PEG chains tethered to the micelle core via pH sensitive hydrazone linkages. Under neutral pH, these 7–15 nm micelles can bind tightly to cell surfaces via the antibody targeting, aiding in micelle accumulation at tumor sites. At low pH environments, shedding of many of the PEG chains led to 'de-shielding' the secondary ligand, which induces delivery of the payload to desired sites within the cell, such as the nucleus. Chemical availability of the antibody was preserved at both pH 8.0 and 5.0 as determined by ELISA assay. Biotin was used as a model 'hidden function,' and micelle retention in an avidin column showed the shielding effects. These dual-targeted micelles showed small amounts of retention in avidin columns (15%), however, when incubated at pH 5.0 for 15 min before column exposure, micelle retention increased to 75%, demonstrating deshielding of the biotin allowing for binding. Similar experiments using the TATp moiety as a hidden ligand demonstrated this effect in cancer cell lines. In both the cases of micelles and liposomes, little or no cell uptake was observed with the shielded systems, but short incubations (30 min) at pH 5.0 resulted in de-shielding and visible increase in uptake as detected by fluorescence microscopy.

A tri-functional micelle design has also been recently published (128). This design carries ligand targeting, pH

sensitivity, and image contrast. Gao *et al*. incorporated superparamagnetic iron oxide (SPIO) nanoparticles into a doxorubicin loaded, cRGD targeted, PEG-PLA micelle. The resulting 46 nm micelles enhanced cell specificity and uptake due to the cRGD ligand, demonstrated pH-triggered release of doxorubicin, and achieved MRI ultrasensitivity. In this case, increased cell uptake could be measured via flow cytometry, a method that can only be used *in vitro*, as well as via magnetic resonance imaging in tumor-bearing animals *in vivo*. This micelle design has the capability of not only treating tumors, but also being imaged non-invasively *in vivo*, so that micelle deposition can be correlated to tumor regression.

CONCLUSION AND FUTURE DIRECTIONS

Polymer micelles are becoming a powerful nanotherapeutic platform that affords several advantages for cancer-targeted drug delivery, including increased drug solubilization, prolonged blood half-lives, preferential accumulation in tumor sites, and a decrease in toxic side effects. Even in their simplest form, when a chemotherapeutic agent is solubilized in the micelle core, micelles have shown marked benefits to cancer therapy. However, the technology is still lacking in tumor specificity and controlled release of the entrapped agents. Hence, the focus has gradually shifted from passive targeting micelles to active targeting and responsive systems that carry additional mechanisms to aid in micelle accumulation at the site of action as well as site-specific release. The picture of the ideal micelle delivery system harkens back to the original vision of Paul Ehrlich's 'magic bullet' more than 100 years ago, where an agent introduced into the bloodstream is able to selectively target diseased tissue while leaving healthy tissue untouched. Great strides in cancer biology have yielded numerous new cancer-specific molecular targets that distinguish tumors from normal tissue. Despite these advances, cancer is an extremely heterogeneous disease and its treatment will likely involve a multifaceted approach rather than a single functionality. The previously discussed ligand targeted, pH sensitive formulations are promising examples of how micelle multifunctionality can lead to a fusion of chemical customization with biological insight so as to exploit multiple routes for tumor treatment. In the years to come, it is expected that knowledge gained in cancer biology and polymer chemistry will catalyze the further development of novel multifunctional micellar systems with greater customization to achieve more efficacious anti-tumor response.

ACKNOWLEDGEMENT

We thank the National Institutes of Health (R01-CA-90696 and R21-EB-005394) for their financial support. NN acknowledges the Royal Thai Government for a predoctoral fellowship support. EB acknowledges the predoctoral support from the NCI Minority Supplement Program. This is manuscript CSCNP008 from the "Cell Stress and Cancer Nanomedicine" program in the Simmons Comprehensive Cancer Center at the University of Texas Southwestern Medical Center at Dallas.

REFERENCES

1. S. Danson, D. Ferry, V. Alakhov, J. Margison, D. Kerr, D. Jowle, M. Brampton, G. Halbert, and M. Ranson. Phase I dose escalation and pharmacokinetic study of pluronic polymer-bound doxorubicin (SP1049C) in patients with advanced cancer. *Br. J. Cancer* **90**:2085–2091 (2004).
2. Y. Matsumura, T. Hamaguchi, T. Ura, K. Muro, Y. Yamada, Y. Shimada, K. Shirao, T. Okusaka, H. Ueno, M. Ikeda, and N. Watanabe. Phase I clinical trial and pharmacokinetic evaluation of NK911, a micelle-encapsulated doxorubicin. *Br. J. Cancer* **91**:1775–1781 (2004).
3. T. Y. Kim, D. W. Kim, J. Y. Chung, S. G. Shin, S. C. Kim, D. S. Heo, N. K. Kim, and Y. J. Bang. Phase I and pharmacokinetic study of Genexol-PM, a cremophor-free, polymeric micelle-formulated paclitaxel, in patients with advanced malignancies. *Clin. Cancer Res.* **10**:3708–3716 (2004).
4. Y. Kakizawa and K. Kataoka. Block copolymer micelles for delivery of gene and related compounds. *Adv. Drug Deliv. Rev.* **54**:203–222 (2002).
5. V. P. Torchilin. Structure and design of polymeric surfactant-based drug delivery systems. *J. Control. Release* **73**:137–172 (2001).
6. M. Jones and J. Leroux. Polymeric micelles—a new generation of colloidal drug carriers. *Eur. J. Pharm. Biopharm.* **48**:101–111 (1999).
7. A. V. Kabanov, P. Lemieux, S. Vinogradov, and V. Alakhov. Pluronic((R)) block copolymers: novel functional molecules for gene therapy. *Adv. Drug Deliv. Rev.* **54**:223–233 (2002).
8. G. S. Kwon and K. Kataoka. Block-Copolymer Micelles as Long-Circulating Drug Vehicles. *Adv. Drug Deliv. Rev.* **16**:295–309 (1995).
9. G. S. Kwon. Polymeric micelles for delivery of poorly water-soluble compounds. *Crit. Rev. Ther. Drug Carr. Syst.* **20**:357–403 (2003).
10. V. P. Torchilin. Block copolymer micelles as a solution for drug delivery problems. *Expert Opin. Ther. Pat.* **15**:63–75 (2005).
11. V. P. Torchilin. Targeted polymeric micelles for delivery of poorly soluble drugs. *Cell Mol. Life Sci.* **61**:2549–2559 (2004).
12. G. Gaucher, M. H. Dufresne, V. P. Sant, N. Kang, D. Maysinger, and J. C. Leroux. Block copolymer micelles: preparation, characterization and application in drug delivery. *J. Control. Release* **109**:169–188 (2005).
13. V. P. Torchilin. Micellar nanocarriers: pharmaceutical perspectives. *Pharm. Res.* **24**:1–16 (2007).
14. A. Choucair and A. Eisenberg. Control of amphiphilic block copolymer morphologies using solution conditions. *Eur. Phys. J., E* **10**:37–44 (2003).
15. A. Choucair and A. Eisenberg. Interfacial solubilization of model amphiphilic molecules in block copolymer micelles. *J. Am. Chem. Soc.* **125**:11993–12000 (2003).
16. Y. S. Yu, L. F. Zhang, and A. Eisenberg. Morphogenic effect of solvent on crew-cut aggregates of apmphiphilic diblock copolymers. *Macromolecules* **31**:1144–1154 (1998).
17. H. W. Shen, L. F. Zhang, and A. Eisenberg. Multiple pH-induced morphological changes in aggregates of polystyrene-block-poly(4-vinylpyridine) in DMF/H2O mixtures. *J. Am. Chem. Soc.* **121**:2728–2740 (1999).
18. P. Dalhaimer, F. S. Bates, H. Aranda-Espinoza, and D. Discher. Synthetic cell elements from block copolymers—hydrodynamic aspects. *Comptes Rendus. Physique* **4**:251–258 (2003).
19. P. Dalhaimer, A. J. Engler, R. Parthasarathy, and D. E. Discher. Targeted worm micelles. *Biomacromolecules* **5**:1714–1719 (2004).
20. P. Dalhaimer, F. S. Bates, and D. E. Discher. Single molecule visualization of stable, stiffness-tunable, flow-conforming worm micelles. *Macromolecules* **36**:6873–6877 (2003).
21. A. Benahmed, M. Ranger, and J. C. Leroux. Novel polymeric micelles based on the amphiphilic diblock copolymer poly(N-vinyl-2-pyrrolidone)-block-poly(D,L-lactide). *Pharm. Res.* **18**:323–328 (2001).
22. J. E. Chung, M. Yokoyama, T. Aoyagi, Y. Sakurai, and T. Okano. Effect of molecular architecture of hydrophobically modified poly(N-isopropylacrylamide) on the formation of

thermoresponsive core-shell micellar drug carriers. *J. Control. Release* **53**:119–130 (1998).
23. J. E. Chung, M. Yokoyama, and T. Okano. Inner core segment design for drug delivery control of thermo-responsive polymeric micelles. *J. Control. Release* **65**:93–103 (2000).
24. J. E. Chung, M. Yokoyama, M. Yamato, T. Aoyagi, Y. Sakurai, and T. Okano. Thermo-responsive drug delivery from polymeric micelles constructed using block copolymers of poly(N-isopropylacrylamide) and poly(butylmethacrylate). *J. Control. Release* **62**:115–127 (1999).
25. O. Soga, C. F. van Nostrum, M. Fens, C. J. Rijcken, R. M. Schiffelers, G. Storm, and W. E. Hennink. Thermosensitive and biodegradable polymeric micelles for paclitaxel delivery. *J. Control. Release* **103**:341–353 (2005).
26. K. Kataoka, G. S. Kwon, M. Yokoyama, T. Okano, and Y. Sakurai. Block copolymer micelles as vehicles for drug delivery. *J. Control. Release* **24**:119–132 (1993).
27. G. S. Kwon, M. Yokoyama, T. Okano, Y. Sakurai, and K. Kataoka. Enhanced tumor accumulation and prolonged circulation times of micelle-forming poly(ethylene oxide-aspartate) block copolymer-Adriamycin conjugates. *J. Control. Release* **28**:334–335 (1994).
28. H. Maeda, K. Greish, and J. Fang. The EPR effect and polymeric drugs: a paradigm shift for cancer chemotherapy in the 21st century. *Polymer Therapeutics Ii: Polymers as Drugs, Conjugates and Gene Delivery Systems* **193**:103–121 (2006).
29. K. Mross, P. Maessen, W. J. van der Vijgh, H. Gall, E. Boven, and H. M. Pinedo. Pharmacokinetics and metabolism of epidoxorubicin and doxorubicin in humans. *J. Clin. Oncol.* **6**:517–526 (1988).
30. A. Gabizon, R. Catane, B. Uziely, B. Kaufman, T. Safra, R. Cohen, F. Martin, A. Huang, and Y. Barenholz. Prolonged circulation time and enhanced accumulation in malignant exudates of doxorubicin encapsulated in polyethylene-glycol coated liposomes. *Cancer Res.* **54**:987–992 (1994).
31. P. H. Wiernik, E. L. Schwartz, J. J. Strauman, J. P. Dutcher, R. B. Lipton, and E. Paietta. Phase I clinical and pharmacokinetic study of taxol. *Cancer Res.* **47**:2486–2493 (1987).
32. V. Weissig, K. R. Whiteman, and V. P. Torchilin. Accumulation of protein-loaded long-circulating micelles and liposomes in subcutaneous Lewis lung carcinoma in mice. *Pharm. Res.* **15**:1552–1556 (1998).
33. R. L. Hong and Y. L. Tseng. Phase I and pharmacokinetic study of a stable, polyethylene-glycolated liposomal doxorubicin in patients with solid tumors: the relation between pharmacokinetic property and toxicity. *Cancer* **91**:1826–1833 (2001).
34. J. Cummings and C. S. McArdle. Studies on the *in vivo* disposition of adriamycin in human tumours which exhibit different responses to the drug. *Br. J. Cancer* **53**:835–838 (1986).
35. D. Goren, A. T. Horowitz, D. Tzemach, M. Tarshish, S. Zalipsky, and A. Gabizon. Nuclear delivery of doxorubicin via folate-targeted liposomes with bypass of multidrug-resistance efflux pump. *Clin. Cancer Res.* **6**:1949–1957 (2000).
36. S. D. Weitman, A. G. Weinberg, L. R. Coney, V. R. Zurawski, D. S. Jennings, and B. A. Kamen. Cellular-localization of the folate receptor—potential role in drug toxicity and folate homeostasis. *Cancer Res.* **52**:6708–6711 (1992).
37. J. F. Ross, P. K. Chaudhuri, and M. Ratnam. Differential regulation of folate receptor isoforms in normal and malignant-tissues *in-vivo* and in established cell-lines—physiological and clinical implications. *Cancer* **73**:2432–2443 (1994).
38. H. S. Yoo and T. G. Park. Folate receptor targeted biodegradable polymeric doxorubicin micelles. *J. Control. Release* **96**:273–283 (2004).
39. H. S. Yoo and T. G. Park. Folate-receptor-targeted delivery of doxorubicin nano-aggregates stabilized by doxorubicin-PEG-folate conjugate. *J. Control. Release* **100**:247–256 (2004).
40. E. K. Park, S. Y. Kim, S. B. Lee, and Y. M. Lee. Folate-conjugated methoxy poly(ethylene glycol)/poly(epsilon-caprolactone) amphiphilic block copolymeric micelles for tumor-targeted drug delivery. *J. Control. Release* **109**:158–168 (2005).
41. E. K. Park, S. B. Lee, and Y. M. Lee. Preparation and characterization of methoxy poly(ethylene glycol)/poly(epsilon-caprolactone) amphiphilic block copolymeric nanospheres for tumor-specific folate-mediated targeting of anticancer drugs. *Biomaterials* **26**:1053–1061 (2005).
42. J. A. Varner and D. A. Cheresh. Tumor angiogenesis and the role of vascular cell integrin alphavbeta3. *Important Adv. Oncol.* 69–87 (1996).
43. A. Teti, S. Migliaccio, and R. Baron. The role of the alphaVbeta3 integrin in the development of osteolytic bone metastases: a pharmacological target for alternative therapy? *Calcif. Tissue Int.* **71**:293–299 (2002).
44. C. Ruegg, O. Dormond, and A. Foletti. Suppression of tumor angiogenesis through the inhibition of integrin function and signaling in endothelial cells: which side to target? *Endothelium* **9**:151–160 (2002).
45. J. Wermuth, S. L. Goodman, A. Jonczyk, and H. Kessler. Stereoisomerism and biological activity of the selective and superactive alpha(v)beta(3) integrin inhibitor cyclo(-RGDfV-) and its retro-inverso peptide. *J. Am. Chem. Soc.* **119**:1328–1335 (1997).
46. H. Kessler, B. Diefenbach, D. Finsinger, A. Geyer, M. Gurrath, S. L. Goodman, G. Holzemann, R. Haubner, A. Jonczyk, G. Muller, E. G. von Roedern, and J. Wermuth. Design of superactive and selective integrin receptor antagonists containing the RGD sequence. *Lett. Pept. Sci.* **2**:155–160 (1995).
47. R. Haubner, W. Schmitt, G. Holzemann, S. L. Goodman, A. Jonczyk, and H. Kessler. Cyclic RGD peptides containing beta-turn mimetics. *J. Am. Chem. Soc.* **118**:7881–7891 (1996).
48. R. Haubner, R. Gratias, B. Diefenbach, S. L. Goodman, A. Jonczyk, and H. Kessler. Structural and functional aspects of RGD-containing cyclic pentapeptides as highly potent and selective integrin alpha(v)beta(3) antagonists. *J. Am. Chem. Soc.* **118**:7461–7472 (1996).
49. S. L. Goodman, G. Holzemann, G. A. G. Sulyok, and H. Kessler. Nanomolar small molecule inhibitors for alpha v beta 6, alpha v beta 5, and alpha v beta 3 integrins. *J. Med. Chem.* **45**:1045–1051 (2002).
50. P. C. Brooks, R. A. Clark, and D. A. Cheresh. Requirement of vascular integrin alpha v beta 3 for angiogenesis. *Science* **264**:569–571 (1994).
51. N. Nasongkla, X. Shuai, H. Ai, B. D. Weinberg, J. Pink, D. A. Boothman, and J. M. Gao. cRGD-functionalized polymer micelles for targeted doxorubicin delivery. *Angewandte Chemie-International Edition* **43**:6323–6327 (2004).
52. G. Ashwelland and J. Harford. Carbohydrate-specific receptors of the liver. *Ann. Rev. Biochem.* **51**:531–554 (1982).
53. M. Goto, H. Yura, C. W. Chang, A. Kobayashi, T. Shinoda, A. Maeda, S. Kojima, K. Kobayashi, and T. Akaike. Lactose-carrying polystyrene as a drug carrier—investigation of body distributions to parenchymal liver-cells using I-125 labeled lactose-carrying polystyrene. *J. Control. Release* **28**:223–233 (1994).
54. R. W. Jansen, G. Molema, T. L. Ching, R. Oosting, G. Harms, F. Moolenaar, M. J. Hardonk, and D. K. Meijer. Hepatic endocytosis of various types of mannose-terminated albumins. What is important, sugar recognition, net charge, or the combination of these features. *J. Biol. Chem.* **266**:3343–3348 (1991).
55. J. Kopacek and R. Duncan. Targetable polymeric prodrugs. *J. Control. Release* **6**:315–327 (1987).
56. J. R. Wands and H. E. Blum. Primary hepatocellular carcinoma. *N. Engl. J. Med.* **325**:729–731 (1991).
57. Y. I. Jeong, S. J. Seo, I. K. Park, H. C. Lee, I. C. Kang, T. Akaike, and C. S. Cho. Cellular recognition of paclitaxel-loaded polymeric nanoparticles composed of poly(gamma-benzyl L-glutamate) and poly(ethylene glycol) diblock copolymer endcapped with galactose moiety. *Int. J. Pharm.* **296**:151–161 (2005).
58. K. Yasugi, T. Nakamura, Y. Nagasaki, M. Kato, and K. Kataoka. Sugar-installed polymer micelles: Synthesis and micellization of poly(ethylene glycol)-poly(D,L-lactide) block copolymers having sugar groups at the PEG chain end. *Macromolecules* **32**:8024–8032 (1999).

59. Y. Nagasaki, K. Yasugi, Y. Yamamoto, A. Harada, and K. Kataoka. Sugar-installed block copolymer micelles: their preparation and specific interaction with lectin molecules. *Biomacromolecules* **2**:1067–1070 (2001).
60. E. Jule, Y. Nagasaki, and K. Kataoka. Surface plasmon resonance study on the interaction between lactose-installed poly(ethylene glycol)-poly(D,L-lactide) block copolymer micelles and lectins immobilized on a gold surface. *Langmuir* **18**:10334–10339 (2002).
61. E. Jule, Y. Nagasaki, and K. Kataoka. Lactose-installed poly(ethylene glycol)-poly(d,l-lactide) block copolymer micelles exhibit fast-rate binding and high affinity toward a protein bed simulating a cell surface. A surface plasmon resonance study. *Bioconjug. Chem.* **14**:177–186 (2003).
62. A. V. Kabanov, V. P. Chekhonin, V. Y. Alakhov, E. V. Batrakova, A. S. Lebedev, N. S. Meliknubarov, S. A. Arzhakov, A. V. Levashov, G. V. Morozov, E. S. Severin, and V. A. Kabanov. The neuroleptic activity of haloperidol increases after its solubilization in surfactant micelles—micelles as microcontainers for drug targeting. *FEBS Lett.* **258**:343–345 (1989).
63. V. P. Torchilin, A. N. Lukyanov, Z. Gao, and B. Papahadjopoulos-Sternberg. Immunomicelles: targeted pharmaceutical carriers for poorly soluble drugs. *Proc. Natl. Acad. Sci. USA.* **100**:6039–6044 (2003).
64. C. Tuerkand and L. Gold. Systematic evolution of ligands by exponential enrichment—Rna Ligands to Bacteriophage-T4 DNA-Polymerase. *Science* **249**:505–510 (1990).
65. A. D. Ellingtonand and J. W. Szostak. *In vitro* selection of Rna molecules that bind specific ligands. *Nature* **346**:818–822 (1990).
66. O. C. Farokhzad, S. Y. Jon, A. Khadelmhosseini, T. N. T. Tran, D. A. LaVan, and R. Langer. Nanopartide-aptamer bioconjugates: A new approach for targeting prostate cancer cells. *Cancer Res.* **64**:7668–7672 (2004).
67. O. C. Farokhzad, J. J. Cheng, B. A. Teply, I. Sherifi, S. Jon, P. W. Kantoff, J. P. Richie, and R. Langer. Targeted nanoparticle-aptamer bioconjugates for cancer chemotherapy *in vivo*. *Proc. Natl. Acad. Sci. USA.* **103**:6315–6320 (2006).
68. J. D. Hood, M. Bednarski, R. Frausto, S. Guccione, R. A. Reisfeld, R. Xiang, and D. A. Cheresh. Tumor regression by targeted gene delivery to the neovasculature. *Science* **296**:2404–2407 (2002).
69. T. J. Wickham. Ligand-directed targeting of genes to the site of disease. *Nat. Med.* **9**:135–139 (2003).
70. K. Kunath, T. Merdan, O. Hegener, H. Haberlein, and T. Kissel. Integrin targeting using RGD-PEI conjugates for *in vitro* gene transfer. *J. Gene Med.* **5**:588–599 (2003).
71. P. Erbacher, T. Bettinger, P. Belguise-Valladier, S. M. Zou, J. L. Coll, J. P. Behr, and J. S. Remy. Transfection and physical properties of various saccharide, poly(ethylene glycol), and antibody-derivatized polyethylenimines (PEI). *J. Gene Med.* **1**:210–222 (1999).
72. C. C. Chen and E. E. Dormidontova. Architectural and structural optimization of the protective polymer layer for enhanced targeting. *Langmuir* **21**:5605–5615 (2005).
73. C. Cluzel, F. Saltel, J. Lussi, F. Paulhe, B. A. Imhof, and B. Wehrle-Haller. The mechanisms and dynamics of alpha v beta 3 integrin clustering in living cells. *J. Cell Biol.* **171**:383–392 (2005).
74. K. Engin, D. B. Leeper, J. R. Cater, A. J. Thistlethwaite, L. Tupchong, and J. D. Mcfarlane. Extracellular Ph distribution in human tumors. *Int. J. Hypertherm.* **11**:211–216 (1995).
75. H. S. Yoo, E. A. Lee, and T. G. Park. Doxorubicin-conjugated biodegradable polymeric micelles having acid-cleavable linkages. *J. Control. Release* **82**:17–27 (2002).
76. Y. Bae, S. Fukushima, A. Harada, and K. Kataoka. Design of environment-sensitive supramolecular assemblies for intracellular drug delivery: polymeric micelles that are responsive to intracellular pH change. *Angew. Chem. Int. Ed. Engl.* **42**:4640–4643 (2003).
77. Y. Bae, W. D. Jang, N. Nishiyama, S. Fukushima, and K. Kataoka. Multifunctional polymeric micelles with folate-mediated cancer cell targeting and pH-triggered drug releasing properties for active intracellular drug delivery. *Molecular Biosystems* **1**:242–250 (2005).
78. Y. Bae, N. Nishiyama, S. Fukushima, H. Koyama, M. Yasuhiro, and K. Kataoka. Preparation and biological characterization of polymeric micelle drug carriers with intracellular pH-triggered drug release property: tumor permeability, controlled subcellular drug distribution, and enhanced *in vivo* antitumor efficacy. *Bioconjug. Chem.* **16**:122–130 (2005).
79. E. R. Gillies and J. M. J. Frechet. A new approach towards acid sensitive copolymer micelles for drug delivery. *Chem. Commun.* 1640–1641 (2003).
80. E. R. Gillies and J. M. J. Frechet. pH-responsive copolymer assemblies for controlled release of doxorubicin. *Bioconjug. Chem.* **16**:361–368 (2005).
81. E. R. Gillies, A. P. Goodwin, and J. M. J. Frechet. Acetals as pH-sensitive linkages for drug delivery. *Bioconjug. Chem.* **15**:1254–1263 (2004).
82. H. R. Stapert, N. Nishiyama, D. L. Jiang, T. Aida, and K. Kataoka. Polyion complex micelles encapsulating light-harvesting ionic dendrimer zinc porphyrins. *Langmuir* **16:** 8182–8188 (2000).
83. H. R. Stapert, N. Nishiyama, D. L. Jiang, T. Aida, and K. Kataoka. Poly-ion complex micelles encapsulating light-harvesting ionic Zn porphyrin dendrimers for PDT. *Abstr. Pap.-Am. Chem. Soc.* **219**:U226 (2000).
84. Y. Q. Tang, S. Y. Liu, S. P. Armes, and N. C. Billingham. Solubilization and controlled release of a hydrophobic drug using novel micelle-forming ABC triblock copolymers. *Biomacromolecules* **4**:1636–1645 (2003).
85. E. S. Lee, H. J. Shin, K. Na, and Y. H. Bae. Poly(L-histidine)-PEG block copolymer micelles and pH-induced destabilization. *J. Control. Release* **90**:363–374 (2003).
86. E. S. Lee, K. Na, and Y. H. Bae. Super pH-sensitive multifunctional polymeric micelle. *Nano Lett.* **5**:325–329 (2005).
87. E. S. Lee, K. Na, and Y. H. Bae. Doxorubicin loaded pH-sensitive polymeric micelles for reversal of resistant MCF-7 tumor. *J. Control. Release* **103**:405–418 (2005).
88. E. S. Lee, K. Na, and Y. H. Bae. Polymeric micelle for tumor pH and folate-mediated targeting. *J. Control. Release* **91**:103–113 (2003).
89. D. M. Lynn, M. M. Amiji, and R. Langer. pH-responsive polymer microspheres: rapid release of encapsulated material within the range of intracellular pH. *Angew. Chem. Int. Ed. Engl.* **40**:1707–1710 (2001).
90. A. Potineni, D. M. Lynn, R. Langer, and M. M. Amiji. Poly(ethylene oxide)-modified poly(beta-amino ester) nanoparticles as a pH-sensitive biodegradable system for paclitaxel delivery. *J. Control. Release* **86**:223–234 (2003).
91. D. Shenoy, S. Little, R. Langer, and M. Amiji. Poly(ethylene oxide)-modified poly(beta-amino ester) nanoparticles as a pH-sensitive system for tumor-targeted delivery of hydrophobic drugs. 1. *In vitro* evaluations. *Mol. Pharmacol.* **2**:357–366 (2005).
92. D. Shenoy, S. Little, R. Langer, and M. Amiji. Poly(ethylene oxide)-modified poly(beta-amino ester) nanoparticles as a pH-sensitive system for tumor-targeted delivery of hydrophobic drugs: part 2. *In vivo* distribution and tumor localization studies. *Pharm. Res.* **22**:2107–2114 (2005).
93. K. S. Soppimath, D. C. W. Tan, and Y. Y. Yang. pH-triggered thermally responsive polymer core-shell nanoparticles for drug delivery. *Adv. Mater.* **17**:318+ (2005).
94. J. Taillefer, M. C. Jones, N. Brasseur, J. E. Van Lier, and J. C. Leroux. Preparation and characterization of pH-responsive polymeric micelles for the delivery of photosensitizing anticancer drugs. *J. Pharm. Sci.* **89**:52–62 (2000).
95. J. Taillefer, N. Brasseur, J. E. van Lier, V. Lenaerts, D. Le Garrec, and J. C. Leroux. *In vitro* and *In vivo* evaluation of pH-responsive polymeric micelles in a photodynamic cancer therapy model. *J. Pharm. Pharmacol.* **53**:155–166 (2001).
96. D. Le Garrec, J. Taillefer, J. E. Van Lier, V. Lenaerts, and J. C. Leroux. Optimizing pH-responsive polymeric micelles for drug delivery in a cancer photodynamic therapy model. *J. Drug Target.* **10**:429–437 (2002).
97. H. Hayashi, M. Iijima, K. Kataoka, and Y. Nagasaki. pH-sensitive nanogel possessing reactive PEG tethered chains on the surface. *Macromolecules* **37**:5389–5396 (2004).

98. T. K. Bronich, P. A. Keifer, L. S. Shlyakhtenko, and A. V. Kabanov. Polymer micelle with cross-linked ionic core. *J. Am. Chem. Soc.* **127**:8236–8237 (2005).
99. J. van der Zee. Heating the patient: a promising approach? *Ann. Oncol.* **13**:1173–1184 (2002).
100. J. E. Chung, M. Yamato, T. Aoyagi, M. Yokoyama, Y. Sakurai, and T. Okano. Temperature-responsive polymeric micelles as intelligent drug carriers. *Abstr. Pap.-Am. Chem. Soc.* **216**:U5 (1998).
101. J. E. Chung, M. Yokoyama, T. Aoyagi, Y. Sakurai, and T. Okano. Effect of molecular architecture of hydrophobically modified poly(N-isopropylacrylamide) on the formation of thermoresponsive core-shell micellar drug carriers. *J. Control. Release* **53**:119–130 (1998).
102. J. E. Chung, M. Yokoyama, K. Suzuki, T. Aoyagi, Y. Sakurai, and T. Okano. Reversibly thermo-responsive alkyl-terminated poly(N-isopropylacrylamide) core-shell micellar structures. *Colloids Surf. B, Biointerfaces* **9**:37–48 (1997).
103. X. M. Liu, K. P. Pramoda, Y. Y. Yang, S. Y. Chow, and C. B. He. Cholesteryl-grafted functional amphiphilic poly (N-isopropylacrylamide-co-N-hydroxylmethylacrylamide): synthesis, temperatureresensitivity, self-assembly and encapsulation of a hydrophobic agent. *Biomaterials* **25**:2619–2628 (2004).
104. X. M. Liu, Y. Y. Yang, and K. W. Leong. Thermally responsive polymeric micellar nanoparticles self-assembled from cholesteryl end-capped random poly(N-isopropylacrylamide-co-N,N-dimethylacrylamide): synthesis, temperature-sensitivity, and morphologies. *J. Colloid Interface Sci.* **266:** 295–303 (2003).
105. F. Kohori, K. Sakai, T. Aoyagi, M. Yokoyama, Y. Sakurai, and T. Okano. Preparation and characterization of thermally responsive block copolymer micelles comprising poly(N-isopropylacrylamide-b-DL-lactide). *J. Control. Release* **55**: 87–98 (1998).
106. J. E. Chung, M. Yokoyama, and T. Okano. Inner core segment design for drug delivery control of thermo-responsive polymeric micelles. *J. Control. Release* **65**:93–103 (2000).
107. M. Nakayama and T. Okano. Polymer terminal group effects on properties of thermoresponsive polymeric micelles with controlled outer-shell chain lengths. *Biomacromolecules* **6**:2320–2327 (2005).
108. S. Q. Liu, Y. W. Tong, and Y. Y. Yang. Incorporation and *In vitro* release of doxorubicin in thermally sensitive micelles made from poly(N-isopropylacrylamide-co-N,N-dimethylacrylamide)-b-poly(D,L-lactide-co-glycolide) with varying compositions. *Biomaterials* **26**:5064–5074 (2005).
109. S. Mitragotri. Innovation—Healing sound: the use of ultrasound in drug delivery and other therapeutic applications. *Nature Reviews Drug Discovery* **4**:255–260 (2005).
110. S. Miyazaki, C. Yokouchi, and M. Takada. External control of drug release—controlled release of insulin from a hydrophilic polymer implant by ultrasound irradiation in diabetic rats. *J. Pharm. Pharmacol.* **40**:716–717 (1988).
111. N. Rapoport, W. G. Pitt, H. Sun, and J. L. Nelson. Drug delivery in polymeric micelles: from *in vitro* to *in vivo*. *J. Control. Release* **91**:85–95 (2003).
112. N. Rapoport, A. I. Smirnov, A. Timoshin, A. M. Pratt, and W. G. Pitt. Factors affecting the permeability of Pseudomonas aeruginosa cell walls toward lipophilic compounds: Effects of ultrasound and cell age. *Arch. Biochem. Biophys.* **344**:114–124 (1997).
113. E. Ruel-Gariepy and J. C. Leroux. *In situ*-forming hydrogels—review of temperature-sensitive systems. *Eur. J. Pharm. Biopharm.* **58**:409–426 (2004).
114. A. V. Kabanov, E. V. Batrakova, and V. Y. Alakhov. Pluronic((R)) block copolymers for overcoming drug resistance in cancer. *Adv. Drug Deliv. Rev.* **54**:759–779 (2002).
115. G. A. Husseini, C. M. Runyan, and W. G. Pitt. Investigating the mechanism of acoustically activated uptake of drugs from Pluronic micelles. *BMC Cancer* **2:** (2002).
116. G. A. Husseini, N. Y. Rapoport, D. A. Christensen, J. D. Pruitt, and W. G. Pitt. Kinetics of ultrasonic release of doxorubicin from pluronic P105 micelles. *Colloids Surf., B Biointerfaces* **24**:253–264 (2002).
117. N. Munshi, N. Rapoport, and W. G. Pitt. Ultrasonic activated drug delivery from pluronic P-105 micelles. *Cancer Lett.* **118**:13–19 (1997).
118. N. Y. Rapoport, J. N. Herron, W. G. Pitt, and L. Pitina. Micellar delivery of doxorubicin and its paramagnetic analog, ruboxyl, to HL-60 cells: effect of micelle structure and ultrasound on the intracellular drug uptake. *J. Control. Release* **58**:153–162 (1999).
119. A. Marin, H. Sun, G. A. Husseini, W. G. Pitt, D. A. Christensen, and N. Y. Rapoport. Drug delivery in pluronic micelles: effect of high-frequency ultrasound on drug release from micelles and intracellular uptake. *J. Control. Release* **84**:39–47 (2002).
120. Z. G. Gao, H. D. Fain, and N. Rapoport. Controlled and targeted tumor chemotherapy by micellar-encapsulated drug and ultrasound. *J. Control. Release* **102**:203–222 (2005).
121. G. A. Husseini, D. A. Christensen, N. Y. Rapoport, and W. G. Pitt. Ultrasonic release of doxorubicin from Pluronic P105 micelles stabilized with an interpenetrating network of N,N-diethylacrylamide. *J. Control. Release* **83**:303–305 (2002).
122. J. D. Pruitt, G. Husseini, N. Rapoport, and M. G. Pitt. Stabilization of pluronic P-105 micelles with an interpenetrating network of N,N-diethylacrylamide. *Macromolecules* **33**:9306–9309 (2000).
123. J. D. Pruitt and W. G. Pitt. Sequestration and ultrasound-induced release of doxorubicin from stabilized pluronic P105 micelles. *Drug Deliv.* **9**:253–258 (2002).
124. J. L. Nelson, B. L. Roeder, J. C. Carmen, F. Roloff, and W. G. Pitt. Ultrasonically activated chemotherapeutic drug delivery in a rat model. *Cancer Res.* **62**:7280–7283 (2002).
125. Y. Katayama, T. Sonoda, and M. Maeda. A polymer micelle responding to the protein kinase A signal. *Macromolecules* **34**:8569–8573 (2001).
126. A. Napoli, M. Valentini, N. Tirelli, M. Muller, and J. A. Hubbell. Oxidation-responsive polymeric vesicles. *Nat. Mater* **3**:183–189 (2004).
127. R. M. Sawant, J. P. Hurley, S. Salmaso, A. Kale, E. Tolcheva, T. S. Levchenko, and V. P. Torchilin. "SMART" drug delivery systems: double-targeted pH-responsive pharmaceutical nanocarriers. *Bioconjug. Chem.* **17**:943–949 (2006).
128. N. Nasongkla, E. Bey, J. M. Ren, H. Ai, C. Khemtong, J. S. Guthi, S. F. Chin, A. D. Sherry, D. A. Boothman, and J. M. Gao. Multifunctional polymeric micelles as cancer-targeted, MRI-ultrasensitive drug delivery systems. *Nano Lett.* **6:** 2427–2430 (2006).
129. J. C. Leroux, E. Roux, D. Le Garrec, K. L. Hong, and D. C. Drummond. N-isopropylacrylamide copolymers for the preparation of pH-sensitive liposomes and polymeric micelles. *J. Control. Release* **72**:71–84 (2001).